High-sensitivity Protein Detection Using Immuno-PCR Phage Construct

A Dissertation

Presented to

the Faculty of the Department of Biomedical Engineering

University of Houston

In Partial Fulfillment

of the Requirements for the Degree

Doctor of Philosophy

in Biomedical Engineering

by

Julia Litvinov

May 2013

High-sensitivity Protein Detection Using Immuno-PCR Phage Construct

Julia Litvinov

Approved:

Chair of the Committee
Dr. Richard C. Willson, Professor
Chemical and Biomolecular Engineering

Dr. Metin Akay, Founding Chair
John S. Dunn Endowed Chair Professor
Biomedical Engineering

Dr. Yasemin Akay, Assistant Professor
Biomedical Engineering

Dr. Elebeoba E. May, Associate Professor
Biomedical Engineering

Dr. Paul Ruchhoeft, Associate Professor
Electrical & Computer Engineering

Dr. Suresh K. Khator, Associate Dean
Cullen College of Engineering

Dr. Metin Akay, Founding Chair
Biomedical Engineering

Acknowledgements

First and foremost, I would like to thank my advisor, Prof. Richard Willson, for his insights and leadership that kept my research on track regardless of the challenges or setbacks. I came into the field of biomolecular engineering with almost no knowledge or perspective of what it takes to become proficient to do PhD level research. Looking back, I would have never succeeded without Prof. Willson's guidance and support.

I would like to thank Prof. Uli Strych, my day-to-day mentor, whose advice on how to get things done in the lab, how to interpret the data, and where and how to get missing information has been truly invaluable in achieving my research objectives. I would like to thank Prof. Katerina Kourentzi and Dr. Anna Hagstrom for being great collaborators and for many fruitful discussions including those that required venting after a long day in the lab. I would like to thank all my lab mates for their comradeship and keeping things lively and exciting in the lab.

I am very grateful to all my committee members for their valuable advice in my PhD endeavor. I would like to specifically thank Dr. Metin Akay for being a great department chair and for creating a highly welcoming and intellectually rich atmosphere for graduate students.

Last but not the least, I would like to thank my husband, Dmitri, for his unwavering support during all my years in college, and my children, who showed lots of love even when my interests went beyond the boundaries of their understanding.

High-sensitivity Protein Detection Using Immuno-PCR Phage Construct

An Abstract

of a

Dissertation

Presented to

the Faculty of the Department of Biomedical Engineering

University of Houston

In partial fulfillment

of the Requirements for the Degree

Doctor of Philosophy

in Biomedical Engineering

by

Julia Litvinov

May 2013

Abstract

Advances in the identification of novel biomarkers of cancer and infection are creating an increasing need for detection systems with superior sensitivity. Early detection and identification of infections speeds effective treatment, and cancers for which early diagnostic methods are available have distinctly higher 5-year survival rates than those for which early detection is lacking. Enzyme-linked immunosorbent assays (ELISAs) provide a high level of versatility, but often lack sensitivity for targets in the sub-picomolar concentration range. The current work describes the development of an ultrasensitive immuno-PCR protein detection assay. Bacteriophage biotin-coupled to off-the-shelf antibodies and quantified by real-time PCR are used as the reporter in the assay to detect the Vascular Endothelial Growth Factor (VEGF) in solution. VEGF promotes angiogenesis, is responsible for cell migration, inhibits cell death, and appears at elevated levels in cancer. The general experimental set-up can be modified based on top-down and bottom-up approaches. The top-down approach involves capturing VEGF on particles functionalized with anti-VEGF antibodies, recognition of VEGF by a monoclonal biotinylated antibody, attachment of NeutrAvidin, and the attachment of biotinylated phage onto the NeutrAvidin. The bottom-up approach involves binding a pre-made conjugate of biotinylated phage/NeutrAvidin/biotinylated antibody to VEGF captured on magnetic beads in a one-step reaction. The experiments are performed in phosphate buffer saline (PBS), 20% serum, and 50% bronchoalveolar lavage (BAL). VEGF can be reproducibly detected at concentrations down to 26 fM in PBS, 50% BAL, and 20% serum.

In the second part of this work, VEGF is assayed on the sample-contact component of biosensors, amorphous pinhole-free aluminum oxide (alumina) coated surfaces, which represents an alternative way to detect phage reporters. This protective layer is usually used for insulation purposes in biosensors to protect them from corrosion in liquid, salty environments. Immobilization of biological agents on biosensors is a common practice and was achieved using TESBA–based silane chemistry coupled with protein A/G to properly orient the antibodies on the surface. VEGF is assayed at nano- and picomolar concentrations and the detection limit by ELISA is estimated to be 7.2 pM.

Table of Contents

List of Figures

List of Tables

1 Chapter 1: Introduction

1.1 Overview

The main goal of the work presented in this dissertation is to construct an assay for protein detection and to show that proteins (such as cancer biomarkers) can be detected at very low concentrations in different body fluids (such as serum and BAL). The Theoretical Background gives basic introduction into cancer research; the VEGFA and its isoforms are studied in terms of stability of VEGFA, its secondary and tertiary structures, as well as MEGA5 alignment of the four most abundant human isoforms of VEGF. Lucentis is presented as one of the anti-VEGF antibodies widely used in cancer treatment and compared to other anti-VEGF antibodies. Bacteriophage is introduced as a PCR reporter engineered to display antibodies and be detected by PCR.

The classical approach to phage display is compared with the current approach, where there is no need for cloning and DNA-insertions into the phage's genome. Here, the use of a single-chain displayed polypeptide was utilized for enzymatic biotinylation and then for use in antibody coupling using biotin-avidin chemistry.

Chapter 2 lists all materials and methods that were used for experiments, as well as results and discussion. Those methods are presented in their finalized version. The optimization is explained later in Chapter 2 (ELISA Optimization and PCR assay optimization). Chapter 2 also introduces the three different formats of VEGF detection. The "one-at-a-time" format was performed in the

layers approach, where all the reagents were added one-by-one to the reaction, with washes between layers to remove non-specifically bound molecules. The "avidin-phage" format was performed to modify the "one-at-a-time" format, where stability of particles was reduced after the addition of NeutrAvidin molecules. To account for this, the biotinylated phage molecules were reacted with NeutrAvidin to create the "avidin-phage" molecule and, later, were added to the reaction as one complex. However, the time of the reagent preparation and the sensitivity of the assay required a more sensitive and less time consuming reagent, as explained in "antibody-phage" format section. Here, an immuno-phage particle was made as biotinylated phage / NeutrAvidin / biotinylated antibody. This molecule allowed the development of a rapid protocol for VEGF detection in a one step reaction.

Chapter 3 describes a different approach to VEGF detection. Amorphous pinhole-free alumina surfaces were introduced as being biologically suitable and corrosion resistive to PBS. Using TESBA chemistry, VEGF was attached to the surface through several linkers and assayed in PBS. The resulting outcome of this assay was a colorimetric ELISA. The conclusions and suggestions for future work are included in Chapter 4.

1.2 Introduction

Cancer is one of the major causes of death worldwide and there remains a great need for improved ultrasensitive detection methods, in particular, for early diagnosis and monitoring of residual disease. Early diagnosis has a significant impact on overall survival rates for cancer patients, as tumors diagnosed at

earlier stages are often curable. While breast and prostate cancer, for which established and sensitive early detection methods exist, have 5-year survival rates of 89 and 100%, respectively, that for cancer of the lung and bronchus is only 15% [1]. This survival difference stems from the fact that 60% of breast and 90% of prostate cancers are diagnosed at localized stages, but 75-80% of lung cancers are diagnosed after the tumor has spread either locally or to distant sites. The discovery of useful panels of protein biomarkers for early detection of cancer has been a significant focus of research in the clinical community in the last decades [2-5]. One such promising biomarker is Vascular Endothelial Growth Factor (VEGF) [6].

Immunoassays for the detection of proteins have been available since the 1960s, and, in the form of the enzyme-linked immunosorbent assay (ELISA) have been a valuable tool in biochemical analyses and medical diagnostics. However, standard ELISAs show a narrow dynamic range, and the sensitivity with which the enzyme label can be detected constrains ELISA sensitivity and applicability [7]. Over the last 30 years, improvements in the ultra-sensitive detection of nucleic acids through DNA amplification (e.g., PCR) have revolutionized diagnosis and research, but there is still no direct equivalent for equally sensitive protein detection. The combination of antibody-like molecular recognition with DNA amplification sensitivity is an intuitively attractive concept which has been visited repeatedly since Sano *et al.* coined the term Immuno-PCR in 1992 [8]. In Immuno-PCR, a chimeric molecule consisting of an antibody linked to an amplifiable DNA is used as the primary molecular

recognition element. Immuno-PCR generally achieves a 100-10,000-fold improvement in the detection limit compared to standard ELISAs, but has still failed ubiquitously to establish itself in the analytical laboratory, mainly due to the complicated preparation of immuno-PCR reagents, non-specific binding, and lack of reproducibility [9-11].

More recently, immuno-PCR reagents have been constructed from nanoparticles decorated with antibodies and DNA oligonucleotides, as shown in **Figure 1 (A),** resulting in assays that require fewer steps to detection, and show a lower detection limit [9, 12-14] than ELISA. In an analogous approach, bacteriophage, easily-manipulated viruses that exclusively infect bacteria [15, 16], expressing single-chain antibody fragments, have been used as affinity agents in the detection of Hantavirus where phage were detected by amplification of part of the phage genome, yielding a 10,000-fold lower LOD (10 pg/mL) than the corresponding ELISA [17]. Kim *et al.* have recently described a sensitive immunoassay for small molecule detection using phage-displayed peptides which bind to antibody-analyte complexes coupled to either ELISA-based [18, 19] or real-time PCR-based [20] detection, as shown in **Figure 1 (B)**.

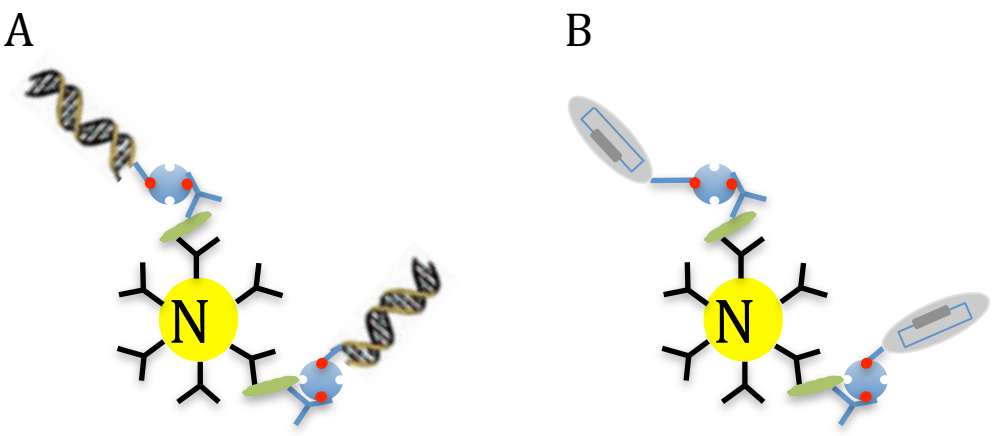

Figure 1: (A) Traditional and (B) phage-based immuno-PCR components. *Magnetic nanoparticles (yellow, NP) are decorated with antibodies (black Y-shaped molecule) for analyte (green oval) capture. The analyte is recognized by the immuno-PCR complex, in which biotinylated detection antibody is attached to (A) a DNA or (B) a phage reporter molecule through streptavidin.*

Here we report an improved modular approach to the previously described immuno-PCR detection assay that employs intact antibodies, (rather than scFvs, which must be cloned and which usually have lower affinity than the parent antibody), avidin-linked to biotinylated bacteriophage, as affinity agents. These AviTag phage used are derivatives of the *Escherichia coli* phage M13 where the N-terminus of the phage coat protein III is replaced by the enzymatically-biotinylatable AviTag peptide (GLNDIFEAQKIEWHE) [21-23]. The lysine residue (K) in the AviTag sequence is a substrate for biotinylation by the *E. coli* biotin ligase (*birA*) enzyme. Using Streptavidin or NeutrAvidin, any biotinylated affinity agent can then easily be linked to these enzymatically biotinylated phage particles.

1.3 Vascular Endothelial Growth Factor

In this work, VEGF was chosen as a model protein analyte. VEGF belongs to the family of platelet-derived growth factors (family of cystine-knot motif) that regulates cell growth and division [24]. When contributing to the cell migration and inhibiting apoptosis by supplying blood and oxygen to various tissues, VEGF can also promote solid cancer growth. For example, the normal brain tissue has approximately from 15 to 50 pg VEGF per mg of tissue and metastatic brain tumor has 332 pg VEGF per mg tissue [25]. Normal levels of VEGF in serum are less than 200 pg/mL, while patients with head and neck squamous cell carcinoma have more than 500 pg/mL [26, 27]. While the method described is a generally applicable platform technology, we decided to validate the performance of this new assay through the detection of this protein. Since VEGF is an established marker for angiogenic activity in cancer, it represents a relevant model protein for developing prognostic and diagnostic assays. In this study we report the detection of VEGF in buffer, serum, and bronchoalveolar lavage fluid (BAL), common background matrices when examining lung cancer patients.

All members of the VEGF family arise from different splicing events of the 8-exon-VEGF gene and have different numbers of amino acids. VEGFA is the best-studied variant and the only member of this family responsible for stimulation of endothelial cell growth [28]. The rest of the paralogs to VEGFA, VEGFB, VEGFC, and VEGFD are placental growth factors [29]; VEGFE is expressed by some viruses, and VEGF-F is found in venom of some snakes [30].

The alternative exon splicing of the VEGF gene resulted in different VEGF isoforms. In humans, the splicing resulted in isoforms VEGFA121, VEGFA145, VEGFA165, VEGFA189, VEGFA206, etc. The most abundant and biologically active form of VEGF in humans is VEGFA165. The gene has a general structure of 8 exons separated by 7 introns. However, VEGF165 does not have the region encoded by exon 6, while VEGF121 lacks the region encoded by both exons 6 and 7. Because of those missing regions, VEGF121 is 44 amino acids shorter than VEGF165. On the other hand, since VEGF165 missing the region of exon 6, it is 24 amino acids shorter than VEGF189 and an additional 17 amino acids shorter than VEGF206. When compared to VEGF165, VEGF206 contains the 41-amino acid insertion, which includes the additional 17 amino acid sequence of VEGF189 [31].

As shown in **Figure 2**, the crystal structure of VEGF reveals that it is a glycosylated disulfide-linked homodimer with seven beta-stranded and two alpha-helical segments. It has a cystine-knot motif that is composed of two disulfide bridges: beta strands 3 and 7 are linked with beta strands 1 and 4 into a ring. Since the VEGF dimer lacks the hydrogen bonds between its beta strands, making the majority of the regions solvent-exposed, this is the only way to stabilize the structure [31-33].

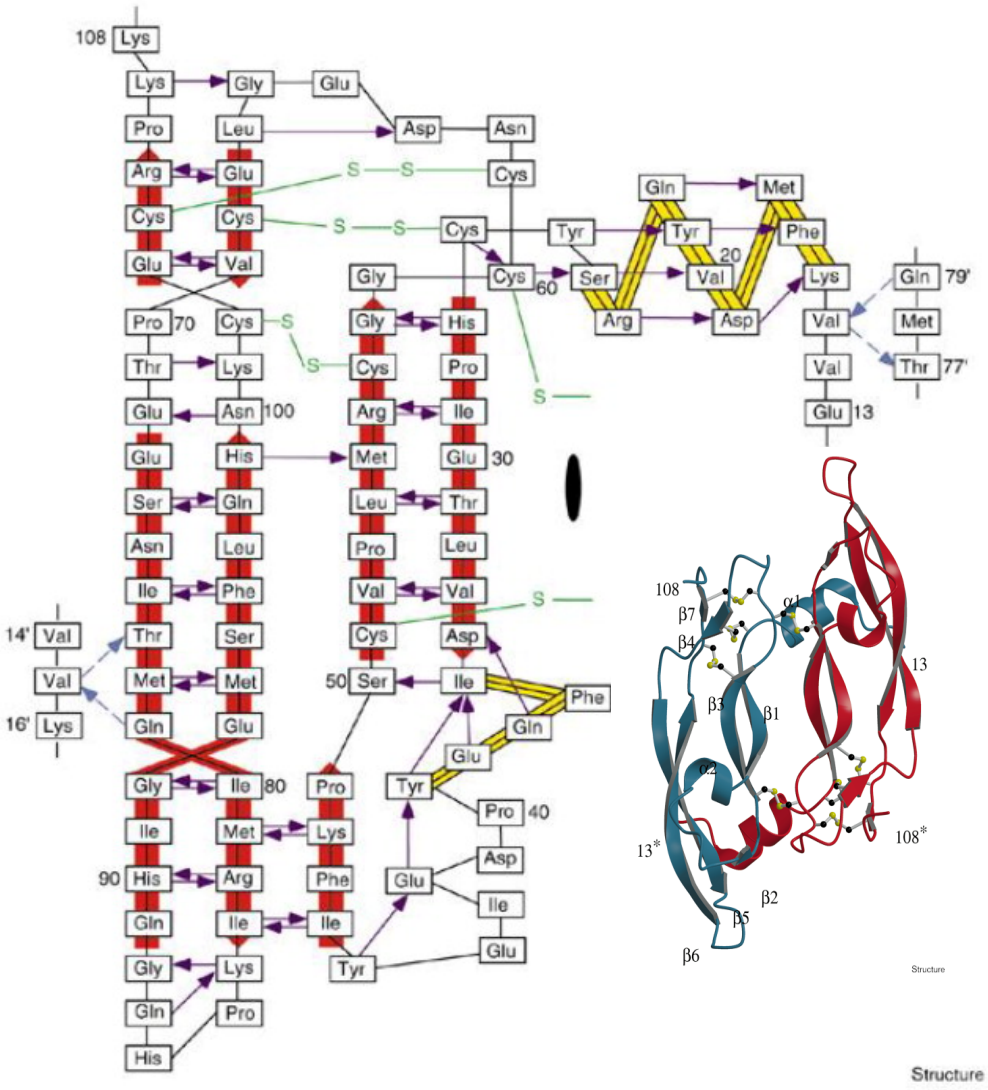

Figure 2: **The structure of VEGF.** *The tertiary structure was determined with a resolution of 1.93 Å [31] and shows the two monomers (red and blue) arranged head-to-tail connected by two disulfide bridges (the sulfur atoms are designated in white and disulfide bonds in yellow). The secondary structure shows the schematic arrangement of amino acids in 2-D structure (green – disulfide bridges, red – beta strands, yellow – helical segments, blue lines – hydrogen bonds) [34].*

As can be seen from **Figure 3**, the MEGA5 alignment of the human VEGFA family corresponds to the literature cited above. The regions of 1-141

and 226-232 amino acid sequence show complete similarity among the 4 main VEGFA isoforms. The only difference is, as shown in the figure (in the exons 6 and 7 regions, amino acid sequences from 142 to 225 including), where the VEGFA 121, 165, and 189 isoforms have partial deletions when compared to the longest VEGFA 206 isoform. This, in turn, implies that there is only one gene responsible for VEGFA synthesis in humans, as also found in literature [24, 34].

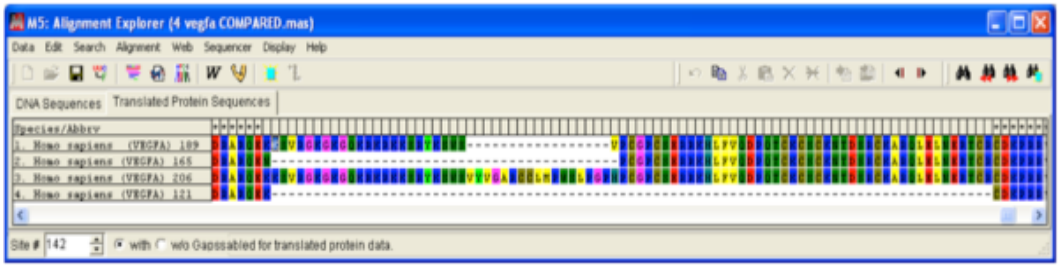

Figure 3: **The regions of differences in amino acid alignment among the human VEGFA isoforms.** *The rest of the alignment shows complete sequence similarity.*

1.4 Lucentis, Avastin, and Macugen as VEGFA recognition antibodies

Lucentis (Ranibizumab) [35] is a prescription medication used to treat macular degeneration, a disease that affects the retina and the back side of the eye leading to gradual loss of vision that obstructs everyday tasks as driving, face recognition, and reading. Lucentis is a Fab-fragment of a recombinant humanized monoclonal antibody Avastin (Bevacizumab) [36], that targets human VEGFA. It binds with equally high affinity to all VEGFA isoforms, thus preventing binding of VEGFA to its receptors [31], and suppressing leakage of blood and inflammation. The molecular weight of Lucentis is 48 kDa and it

consists of a light chain (214 residues) and a heavy chain (231 residues) linked together by a disulfide bond [37].

Avastin, the full-length antibody that Lucentis was derived from (**Figure 4**), is used for treatment of metastatic colorectal cancer, metastatic kidney cancer, glioblastoma, and nonsquamous non-small cell lung cancer. It is a drug that slows the growth of new blood vessels by blocking VEGF from binding to its receptors. Macugen [38], in contrast to Avastin and Lucentis, is not an antibody, but a nucleic acid aptamer. It consists of a chain of single-stranded nucleic acids and, just as Avastin and Lucentis, is designed to recognize human VEGFA.

Lucentis has a 5-fold higher binding affinity to VEGF than Avastin, the full-length antibody that it was derived from. However, Avastin has 2 recognition binding sites for VEGF, while Lucentis has only one [39]. Studies conducted in rabbits show that Lucentis is cleared from the system within 3 days, while it takes the full-length antibody, Avastin, 5.6 days [40].

The majority of this work is based on Lucentis as the VEGF recognition antibody. Lucentis was donated by Dr. William Foster, University of Houston.

The amino acid sequences of the light and heavy chains are:

Light chain:

DIQLTQSPSSLSASVGDRVTITCSASQDISNYLNWYQQKPGKAPKVLIYFT
SSLHSGVPSRFSGSGSGTDFTLTISSLQPEDFATYYCQQYSTVPWTFGQGT
KVEIKRTVAAPSVFIFPPSDEQLKSGTASVVCLLNNFYPREAKVQWKVD
NALQSGNSQESVTEQDSKDSTYSLSSTLTLSKADYEKHKVYACEVTHQG
LSSPVTKSFNRGEC

Heavy chain:

EVQLVESGGGLVQPGGSLRLSCAASGYDFTHYGMNWVRQAPGKGLEW

VGWINTYTGEPTYAADFKRRFTFSLDTSKSTAYLQMNSLRAEDTAVYYC

AKYPYYYGTSHWYFDVWGQGTLVTVSSASTKGPSVFPLAPSSKSTSGGT

AALGCLVKDYFPEPVTVSWNSGALTSGVHTFPAVLQSSGLYSLSSVVTV

PSSSLGTQTYICNVNHKPSNTKVDKKVEPKSCDKTHL

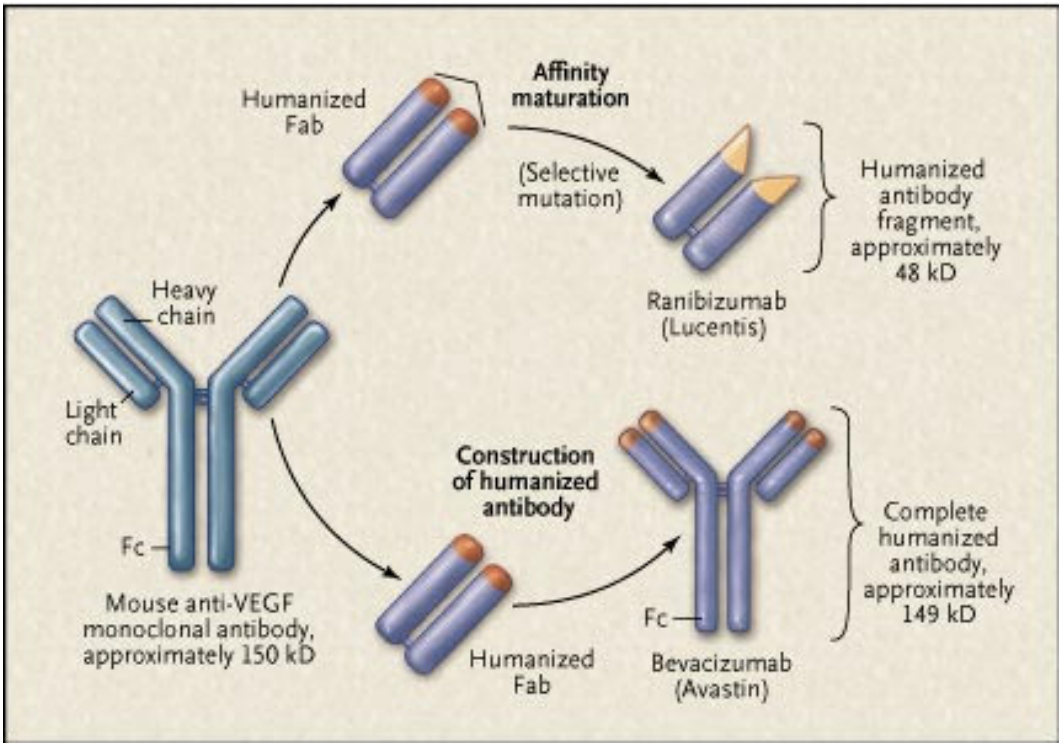

Figure 4: Relationship between Avastin and Lucentis. (Adapted from R. Steinbrook, M.D., " The Price of Sight — Ranibizumab, Bevacizumab, and the Treatment of Macular Degeneration," *N Engl J Med*, Vol. 355, pp. 1409-1412, 2006).

1.5 Bacteriophage M13

Bacteriophage are viruses that infect bacteria. The virus is metabolically inert and can reproduce by infecting the bacterial host [41]. Once the bacteria are infected and phage's genomic material is introduced into the bacterial cell, the progeny phages are produced. The M13 phage, in contrast to other phage, does not kill the bacteria, but continually exits from bacteria, allowing more phage to infect more them. The resulting phage virus is specific for *E. coli*, the Gram-negative bacteria [42, 43]. Filamentous M13 phages are about 900 nm long, approximately 9 nm in diameter, and contain 5 major coat proteins, as shown in **Figure 5** [44, 45].

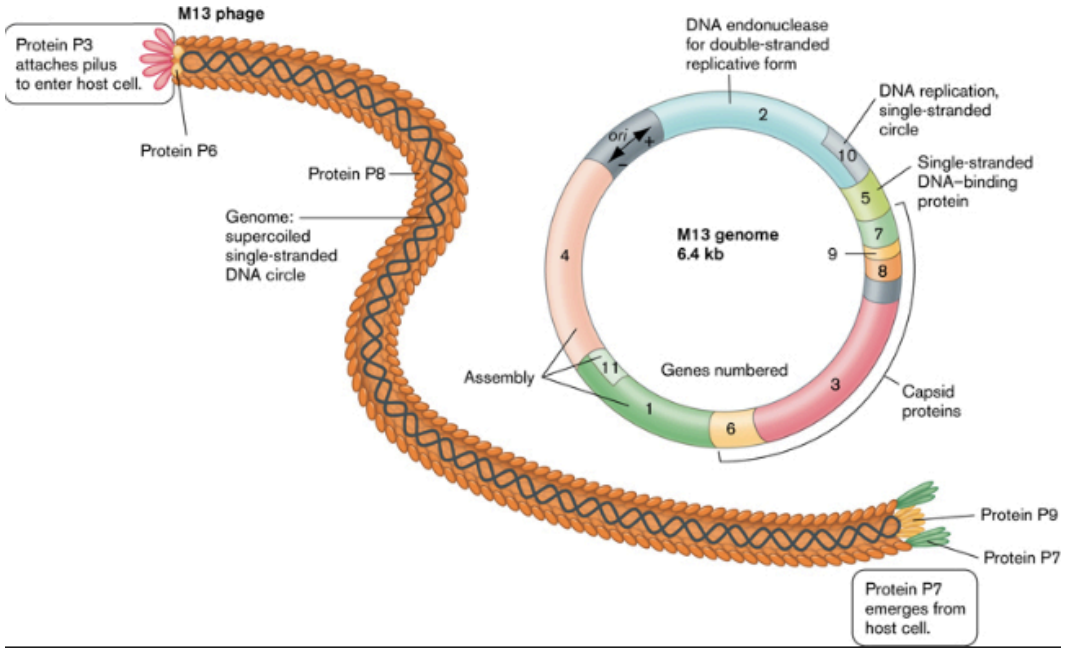

Figure 5: Schematic of a bacteriophage molecule, its DNA structure, and major coat proteins *(adapted from "Molecular Biology Of Viruses", W. W. Norton & Company, Inc., ebook on Microbiology, Second Edition, last accessed online on April 2, 2013).*

1.6 Classical Phage Display Approach

Phage display is a widely used method of testing large libraries of molecules, e.g., antibodies, for their ability to bind to a pre-selected target. The phage physically links each molecule to be tested to the DNA encoding it, which can be read out on the single-phage scale to determine the structure of "winners" after selection among the displayed molecules. The classical approach to the phage display consists of insertion of non-phage DNA fragments into phage genome, making the phage display certain peptide sequences, which may be recognized by other biological agents with high affinity and specificity, as shown in **Figure 6**. Many different types of peptides can be expressed using phage display [46, 47]. The drawback of this genetic fusion approach for developing diagnostics based on a chosen antibody, for example, is that both the peptide and the DNA fragment have to be of a known sequence [48, 49]. If the genetic-fusion display approach is used in diagnostics, the entire sequence of the antibody has to be known [50].

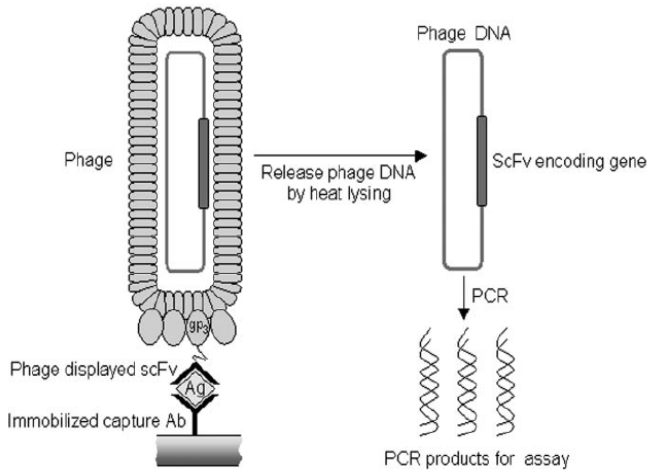

Figure 6: Schematic diagram of genetic-fusion-mediated phage display with PCR readout. *(Adapted from "Phage display mediated immuno-PCR", Yong-*

Chao Guo, Ya-Feng Zhou, Xian-En Zhang, Zhi-Ping Zhang, Yan-Mei Qiao, Li-Jun Bi, Ji-Kai Wen, Mi-Fang Liang and Ji-Bin Zhang, Nucleic Acids Research, v.34, Issue 8, 2006, 10.1093/nar/gkl260.)

1.7 Current Approach

We avoided the need to clone the antibody of interest by using a general platform technology based on phage displaying a single, biotinylatable peptide. Making the phage to express a certain peptide and then altering the displayed peptide enzymatically is a different approach to phage display [51, 52], and very useful for the development of diagnostic assays. In this approach the antibodies to be displayed must simply be biotinylated, not cloned. The major coat protein, pVIII, exists in approximately 2700 copies and occupies most of the length of the phage molecule [53]. Other minor coat proteins (pVII, pIX, for phage assembly and release, pVI and pIII for particle stability and infection) are located at both ends of the phage molecule and are present in very few copies [43, 54, 55].

The primary structure of protein pVIII is responsible for particle properties: the mature version of the gene g8p has 50 amino acids that are arranged in alpha-helical structure, giving rise to a short rod [56]. There are three distinct domains within this gene: a hydrophilic surface comes from the negatively charged amino terminal ends, a positively charged terminal at the carboxyl end, and a hydrophobic region responsible for formation and stabilization of the phage particle.

The genome of M13 phage contains 11 genes, five of which encode for the coat proteins and the other six encode for proteins responsible for replication and virus assembly. The infection of *E. coli* by M13 happens by the formation of

interaction between bacteriophage's coat protein g3p and the *E. coli's* integral membrane protein TolA [57]. Inside *E. coli*, a single-stranded DNA of bacteriophage is converted into a double-stranded DNA, which serves as a template for new single-stranded DNA through replication mode [58]. In contrast to other viruses, the genome of the phage can be successfully packaged with a longer-sequence foreign DNA pieces. However, the higher the increase over the normal genome size, the less efficient becomes the replication of the entire genome [59].

In this light, a short N-terminal AviTag sequence (GLNDIFEAQKIEWHE) [28, 60, 61] was cloned and displayed at the N terminus (SSRP-) of mature protein pIII by the laboratory of Dr. Brian Kay, UIC. This insertion into the phage genome does not affect the stability of the AviTag phages. Furthermore, to overcome the arbitrary uncontrollable biotinylation of other biologically active sites, this peptide allows for site-specific enzymatic biotinylation of the Lysine (K) residue of the sequence. The sequence itself represents a target for biotin ligase BirA enzyme and can be *in vitro* biotinylated in the presence of ATP and biotin. The biotin molecules enable the attachment of any biotinylated molecule via the NeutrAvidin – biotin bridge [29, 61]. The enzymatic attachment of biotin to lysine is covalent [62] and the interaction between avidin and biotin is the strongest among non-covalent attachments known with dissociation constant of 10^{-15} M [63]. The avidin-biotin bond can be used to build modular, custom detection reagents, as shown in **Figure 7**.

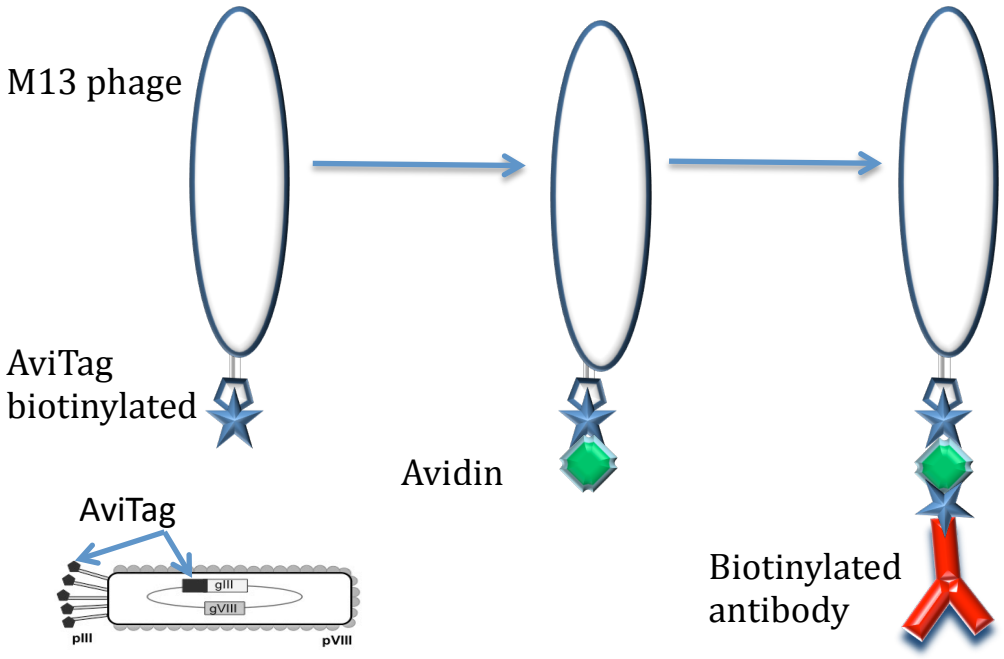

Figure 7: Schematic set-up for modular construction of immuno-phage detection reagents using avidin-biotin chemistry. *(Partially adapted from Scholle et al., ChemBioChem, Vol 7, Issue 5, p. 834-838, 2006).*

2 Chapter 2: Immuno-phage PCR assay

2.1 Materials and Methods

Here we report the development of the novel immuno-detection assay using non-pathogenic bacteriophage easily linkable to common affinity agents, such as antibodies. The principle of the method is shown in **Figure 8.** Initially, antibody-functionalized magnetic capture particles are used to capture and concentrate the analyte from solution. M13 phage engineered to express the AviTag peptide as a *gene III* fusion are enzymatically biotinylated, thus, allowing the attachment of chemically biotinylated antibodies using NeutrAvidin as a linker. This approach yields affinity agents where the binding of an antibody to its target can be ultra-sensitively reported through real-time amplification of the phage genome, with very low non-specific binding, as shown below. We demonstrated the use of these phage immuno-detection reagents in three different formats (Figure 7 and described below), using VEGF as a model analyte.

Unless otherwise specified, reagents were purchased from Sigma-Aldrich (St. Louis, MO). AviTag bacteriophage were a gift from Prof. Brian Kay at the University of Illinois at Chicago. De-identified bronchoalveolar lavage fluid (BAL fluid) samples were provided through an IRB-approved protocol at The Methodist Hospital Research Institute, Houston, TX. The monoclonal anti-VEGF antibody, Lucentis [64] (a G1k isotype antibody fragment, MW of 48 kDa) was a gift from Dr. William Foster, University of Houston.

2.2 "One-at-a-time" format

In this approach, a step-wise process in which each assay component is added to the reaction individually as follows: 100 µL VEGF (BioLegend, (San Diego, CA) Cat. No. 584502; 2.6 nM, serially diluted 10-fold in PBS) were mixed in PBS with magnetic particles (0.5 µg; ~$5*10^6$) functionalized with polyclonal anti-VEGF antibodies, and incubated on an orbital shaker for 2 h at 25°C. The particles were concentrated with a magnet and washed three times with PBS, resuspended in 100 µL PBS containing 200 pM biotinylated antibody, and allowed to incubate for 2 h at 25°C on an orbital shaker. The particles were then washed as above, resuspended in 100 µL PBS containing 170 pM NeutrAvidin and incubated for 30 min. After another wash, the particles were resuspended in 100 µl PBS containing 60 pM biotinylated phage and incubated for 4 h at 25°C. After two washes with 0.3% Tween 20 in PBS to remove unbound phage and two washes with PBS, the particles were analyzed by PCR.

2.3 "Avidin-phage" format

In this approach, VEGF is first captured onto antibody-functionalized magnetic particles before the second biotinylated antibody and pre-assembled NeutrAvidin/biotinylated phage reagent are added for detection. 100 µL VEGF from 26 pM to 26 aM were mixed (in PBS, 20% bovine serum (Life Technologies), or 50% BAL fluid) with magnetic particles (0.5 µg; ~$5*10^6$) functionalized with polyclonal anti-VEGF antibodies, and incubated on an

orbital shaker for 2 h at 25°C. The NeutrAvidin/biotinylated phage (60 pM) and free biotinylated Lucentis (2 nM) were added to the reaction simultaneously (final volume 100 µL). The reaction was allowed to incubate for 4 h at 25°C on an orbital shaker. After two washes with 0.3% Tween 20 in PBS to remove unbound phage and two washes with PBS, the particles were analyzed by PCR.

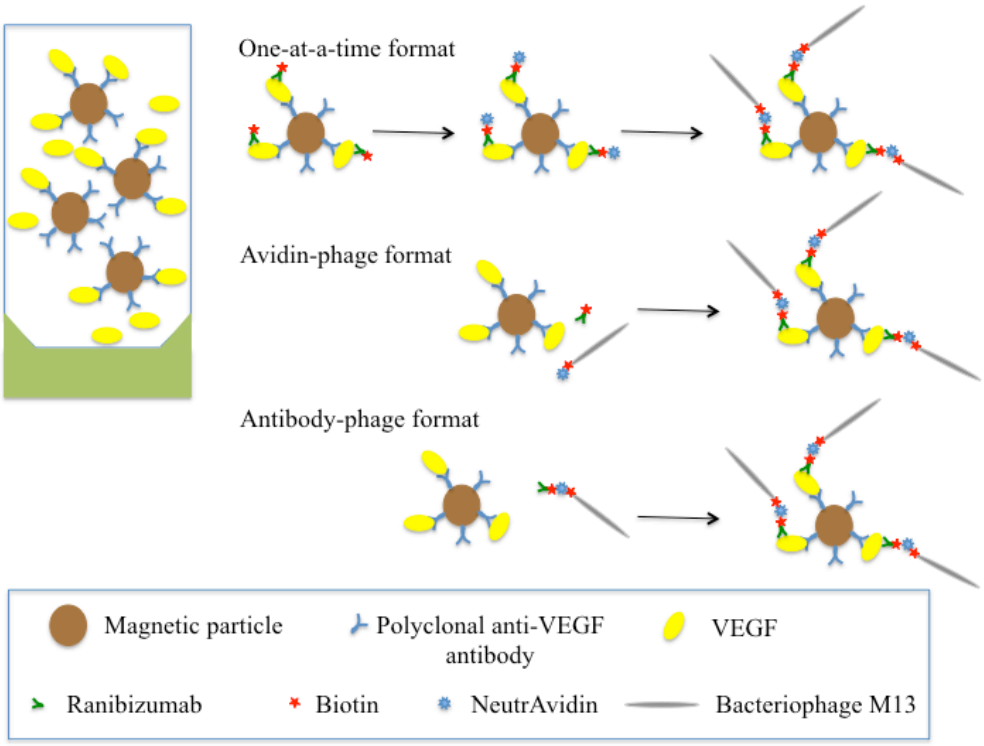

Figure 8: **Schematic of the different immuno-phage approaches.** *One-at-a-time: reagents are added one-by-one to the magnetic capture particles with washes after every step. Avidin-phage: biotinylated phage/NeutrAvidin complexes are pre-made and added as the last step. Antibody-phage: biotinylated phage/NeutrAvidin/biotinylated Lucentis complexes are pre-made and added to VEGF captured on magnetic particles.*

2.4 "Antibody-phage" format

In this approach, antibody-functionalized magnetic capture particles were incubated with VEGF, washed, and then the complete pre-made immuno-phage

reagent of biotinylated antibody/NeutrAvidin/biotinylated phage was added for detection. 100 µL VEGF at concentrations from 26 pM to 260 aM (in PBS, 20% bovine serum, or 50% BAL fluid) were mixed with magnetic particles (0.5 µg, ~5*10^6) functionalized with the polyclonal anti-VEGF antibody, incubated on a shaker for 2 h at 25°C and then washed three times with PBS. The particles were then incubated with 100 µL 3% (w/v) BSA in PBS for 2 h at 25°C, washes three times with PBS, and the antibody/NeutrAvidin/biotinylated phage construct was then added to the reaction at 60 pM, and the reaction was allowed to incubate for 2 h at 25°C on a shaker. After two washes with 0.3% (v/v) Tween 20 in PBS to remove unbound phage and two washes with PBS, the particles were analyzed by PCR.

2.5 PCR

After the final wash of the captured immuno-phage constructs, the magnetic particles were resuspended in 20 µL PBS. 15 µL PCR master mix (0.1 µL of 10 µM forward primer, 0.1 µL of 10 µM reverse primer, 10 µL of 2xPCR mix (Brilliant III Ultra-Fast SYBR mix, Agilent, Santa Clara, CA) and 4.8 µL of RNase- and DNase- free DI water) were added to 5 µL of each sample to achieve 20 µL total PCR volume.

The number of retained phage particles was determined by PCR against a standard curve derived from a 10-fold dilution series (10^{11} to 10^5 phage/mL). The AviTag-targeting PCR primers were as following: *Forward*: 5'-GTTGTTTCTTTCTATTCTCACT-3' and *Reverse*: 5'-

CAGACGTTAGTAAATGAATTTT-3'. The PCR conditions were: 10 min at 95°C, 40 cycles of 30 sec at 62°C and 30 sec at 72°C, followed by the dissociation step (1 min at 95°C, 30 sec at 55°C, and 30 sec at 55°C).

2.6 Preparation of reagents and assay components

2.6.1 Preparation of antibody reagents

The biotinylation of the antibodies used in this study was performed using the EZ-Link™ Sulfo-NHS-SS-Biotin Kit (Thermo Scientific, (Barrington IL)) as described in the manufacturer's protocol. The reaction was allowed to proceed for 1 h before unincorporated biotin was removed using 7 kDa Zeba™ spin desalting columns (Thermo Scientific). The degree of biotinylation was estimated using 4'-hydroxyazobenzene-2-carboxylic acid (HABA, Thermo Scientific). The HABA dye binds to avidin to produce a yellow-orange colored complex and the bound HABA molecule absorbs at 500 nm (with a known extinction coefficient). A solution containing the biotinylated antibody is added to a solution containing the HABA/avidin mixture. Biotin has a higher affinity for avidin and thus displaces HABA. The resulting decrease in the HABA molecule absorbance at 500 nm is used to estimate the degree of antibody biotinylation. The concentration of antibody in the final solution is calculated in mmol/mL, dividing the mg/ml concentration of the antibody solution by the typical molecular weight of an IgG antibody (150,000 g/mol). The concentration of biotin was calculated by dividing the delta OD by the extinction coefficient (34,000 /M/cm) of the HABA/avidin molecule. To calculate the number of the

biotin molecules per one antibody molecule, the molar concentration of biotin was divided by the molar concentration of antibody.

2.6.2 Capture particle functionalization

2.6.2.1 One micron Dynabeads® MyOne ™

Magnetic capture particles (20 µL, ~10^9 Dynabeads® MyOne ™ (1 µm), Tosyl-activated, Life Technologies, Grand Island, NY) were antibody-modified according to the manufacturer's protocol. The particles were washed, resuspended in coating buffer (1x10^7 particles in 1 mL 0.1 M sodium borate, pH 9.5) and mixed with 240 µL polyclonal anti-human VEGF antibody (0.1 mg/mL, R&D Systems, AB-293-NA) and 240 µL of 3 M ammonium sulfate ($(NH_4)_2SO_4$). After 24 h incubation at 37°C with slow tilt rotation, the particles were collected and resuspended in 500 µL of phosphate-buffered saline (PBS) containing 0.5% (w/v) Bovine Serum Albumin (BSA) and 0.05% (v/v) Tween 20 and incubated for 24 h at 37°C. The particles were then washed three times with 1 mL PBS containing 0.1% (w/v) BSA and 0.05% (v/v) Tween 20, and finally resuspended and stored in 200 µL PBS containing 0.1% (w/v) BSA.

2.6.2.2 NanoMag carboxyl particles, 250 nm

Magnetic capture particles (Micromode Partikeltechnologie GmbH, NanoMag 650.12) were antibody-modified according to the manufacturer's protocol (EDAC method). 12 mg EDAC and 24 mg NHS were dissolved in 2 mL 0.5M MES buffer (pH 6.3). 10 mL of 250 nm NanoMag carboxyl particles were added to the solution and incubated for 1 hour with continuous mixing at room

temperature. The particles were washed 3 times with 0.1 M MES buffer and re-suspended in 960 μL of 0.1 M MES buffer and 40 μL of 1 mg/ml of polyclonal anti-human VEGF antibody (R&D Systems, AB-293-NA) after which, the reaction was incubated at 25°C for 3 h with continuous mixing. Without washing, 1 ml of 25 mM glycine in 1xPBS was added to the particles and the incubation continued for 30 more minutes at room temperature with mixing. The particles were washed 3 times with 1xPBS and resuspended and stored in 10 mL 1xPBS.

2.6.3 Growth of AviTag Phage

The TG1 strain of *E. coli* was grown on a fresh M9 plate overnight. A single plaque was picked and incubated in 5 mL of LB medium at 37 °C for 5 h until mid-log phase. The pre-culture was infected with a single Avitag phage colony (or with 5 μL of liquid phage stock) and grown for 2 h at 37 °C. The pre-culture was transferred into 500 mL 2xTY medium in a 2 L flask and grown overnight. The phages were harvested by centrifugation, the pellet containing *E. coli* was discarded, leaving phage in the medium. The medium was filtered and phage was precipitated out of solution with 20% PEG in 2.5M NaCl. The liquid was centrifuged again and the phage pellet was re-suspended in 1 mL of PBS. The final phage solution was filtered through 0.45 μm syringe filter to remove the remaining *E. coli* cell debris. If the phage stock is too thick, one mL (or more) of PBS can be added to the solution before filtering. This step should be followed by additional PEG precipitation. Twenty-five μg/μL of ampicillin and sodium azide to the final concentration of 0.02% by volume were added to the

filtered phage stock. At this point, phage was titered to determine the number of phages per mL.

2.6.4 Biotin ligase preparation

Biotin ligase preparation was performed by Mohan Vivek of the Willson lab as previously described in the literature [16]. AviTag phage were biotinylated using biotin ligase, expressed and purified from *E. coli,* harboring pET14v_SUMO-birA, a gift from Prof. Brian Kay. The enzyme was expressed as inclusion bodies from cells (4 L) grown in the *Overnight Express Autoinduction System 1* (Novagen, Madison, WI). The cells were harvested by centrifugation (30 min, 3,000 x g, 4°C), washed in 50 mL TBS (20 mM Tris-HCl, pH 8, 150 mM NaCl), and resuspended in 150 mL resuspension buffer (20 mM Tris-HCl, pH 8, 10 mM β-mercaptoethanol). After a 1 h incubation at 4°C with 0.1 mg/ml lysozyme (Sigma-Aldrich) and 1.25% (v/v) Serratia Nuclease, [32] the cells were sonicated for 5 min, and 2 ml 70% NP-40 solution, and 40 ml B-PER (Thermo-Fisher) were added. After 1 h at 4°C, the cell lysate was centrifuged (30 min, 16,000 x g, 4°C), and the pellet containing the inclusion bodies was denatured using 7.5 M urea, 0.4 M L-arginine, 10 mM DTT, 50 mM Tris-HCl, pH 8, 500 mM NaCl. The inclusion bodies were refolded in 50 mM Tris-HCl, pH 8, 500 mM NaCl, 5 % (v/v) glycerol, 5% (v/v) sucrose), and applied to a chelating Sepharose column charged with 0.1 M $NiSO_4$. The hexahistidine-tagged biotin ligase was eluted using an imidazole gradient (0.02-0.25 M). Peak fractions were checked for homogeneity using SDS-PAGE.

2.6.5 Phage biotinylation

100 µL of 10^{11} phage/mL were mixed with 14.3 µL Bicine (0.5 M, pH 8.3), 14.3 µL of a solution containing 100 mM ATP, 100 mM $MgO(Ac)_2$ and 500 µM Biotin, 10 µL D-biotin (500 µM), (Avidity), and 10 µL biotin ligase (2 mg/ml) in Tris-HCl, pH 8 and incubated for 1 h at 25°C. Phage were precipitated from the reaction by adding 250 µL of 20% PEG in 2.5 M NaCl to 1 mL of biotinylated phage, followed by 1 h incubation on ice, and centrifugation at 11,000 x g for 20 min. The phage pellet was resuspended in 1 mL PBS.

The efficiency of phage biotinylation was estimated by ELISA using Streptavidin-coated microtiter plates (StreptaWell High Bind, Roche Applied Science, (Indianapolis, IN)). Phage dilutions (10^{11} to 10^5 phage/mL, 100 µL) were added to Streptavidin pre-coated wells and incubated on an orbital shaker for 1 h at 25°C. The wells were then washed three times with 300 µL PBS on a Tecan Hydroflex microplate washer. An HRP/anti-M13 monoclonal antibody conjugate (cat 27-9421-01, GE Healthcare Life Sciences, Pittsburgh, PA) was then added (100 µL/well, 1:5000 diluted in 1xPBS) and incubated for 1 h on a platform shaker at 25°C. Wells were washed three times with 300 µL PBS before 100 µL 1-Step™ Ultra TMB-ELISA Substrate (Thermo Scientific) was added. The reaction was stopped after 20 min with 50 µL 2 M H_2SO_4 and absorbance was measured at 450 nm in a Tecan Infinite M200Pro microplate reader.

2.6.6 NeutrAvidin/biotinylated phage complex preparation

To prepare the NeutrAvidin/biotinylated phage construct, NeutrAvidin (A-2666, Life Technologies) and biotinylated phage were incubated at a molar

ratio of 100:1 in 500 µL PBS, pH 7.7 on a rotary mixer for 40 min at 25°C. Unincorporated NeutrAvidin was removed using an Amicon 100 kDa centrifugal filter (Millipore, Billerica, MA) according to the manufacturer's instructions. Phage were collected in a final volume of 20 µL and stored at 4°C.

2.6.7 Biotinylated antibody/NeutrAvidin/biotinylated phage complex preparation

To prepare the antibody/NeutrAvidin/biotinylated phage construct, the biotinylated Lucentis and NeutrAvidin/biotinylated phage were mixed at a molar ratio of 10:1 in 500 µL of PBS, pH 7.7, and incubated for 24 h at 25°C with continuous rotation. Then, free antibodies were removed using an Amicon 100 kDa filter as described above. The concentrated Lucentis/NeutrAvidin/biotinylated phage construct (10^{11} phage constructs/mL) was stored at 4°C, and was diluted just prior to use.

2.7 Antibody characterization and qualification by ELISA

The performance of the immuno-phage PCR assay depends critically on the quality and performance of the antibodies used. Initially, a VEGF ELISA immunoassay was first performed to determine which reagents to use, their quantity, times of incubation, assay buffers and blocking buffers.

2.7.1 Confirmation of biotinylation of Lucentis

One hundred µL of stock Lucentis and 100 µL of biotinylated Lucentis in 10-fold dilutions from 2 nM to 20 fM, and zero (n=2 for each), were adsorbed on

a standard ELISA plate (Medisorb, 96-well, NUNC) for 2 h at 25°C on a shaker, then washed 3 times with PBS and then the wells were blocked with 300 µL 3% BSA for 2 h at 25°C on a shaker. After three washes with PBS, 100 µL of HRP-labeled Streptavidin was incubated in 1:500 dilution (1 µg/mL, catalog number SNN1004, Invitrogen) for 1 hour and washed 3 times with PBS. One hundred µL of 1-Step™ Ultra TMB-ELISA substrate was added to the wells and allowed to develop for 35-40 min (the reaction was extremely slow). Then, 50 µL of 2 M H_2SO_4 were added to stop the reaction and the OD values were measured with plate reader at 450 nm.

2.7.2 Detection of VEGF with HRP-labeled antibody by conventional ELISA

Since the performance of any immunological assay depends upon the affinity reagents used, the limit of detection of a standard sandwich ELISA using the same anti-VEGF antibodies as used in the immuno-phage assay was first determined. Polyclonal anti-VEGF antibody (100 µL/well of 6.7 nM) was adsorbed on a standard ELISA plate (Medisorb, 96-well, NUNC) for 2 h. The plate was washed three times with PBS on a Tecan Hydroflex microplate washer, and blocked with 3% BSA in PBS for 1 h followed by one PBS wash. VEGF (diluted in PBS from 2.6 nM to 2.6 fM) was incubated in the wells for 2 h. After the wash, monoclonal anti-VEGF antibody (100 µL/well of 2 nM Lucentis) or biotinylated monoclonal anti-VEGF antibody (100 µL/well of 2 nM Lucentis) was added, incubated 2 h and washed three times with PBS. An HRP-labeled rabbit anti-human antibody (100 µL/well, 1:5000 diluted; Santa Cruz

Biotechnology, sc-2769) or HRP-labeled streptavidin (100 µL/well, 1:500 diluted, 1 µg/mL, catalog number SNN1004, Invitrogen) was added respectively, incubated for 1 h, washed three times with PBS and 100 µL 1-Step™ Ultra TMB-ELISA Substrate (Thermo Scientific) were added to the wells. The reaction was stopped with 50 µL 2 M H_2SO_4 and absorbance was measured at 450 nm in a Tecan Infinite M200Pro microplate reader. All incubations were performed at 25°C on an orbital shaker.

The ELISA was also a convenient way to investigate the effect of different blocking reagents on the VEGF detection assay, keeping in mind potential differences between ELISA plates and magnetic particles. For this purpose, we investigated the use of 3% Blotto (Blotto, non-fat dry milk, catalog number sc-2325, Santa Cruz Biotechnology, Inc.) and 3% BSA in PBS microwell after the VEGF incubation step. The procedure followed was as described in Section 2.3.4.

2.7.3 ELISA for phage-mediated VEGF immunoassay with Avastin and Lucentis

VEGF in PBS, 26 nM, was adsorbed on select wells for 2 h of a standard ELISA plate (Medisorb, 96-well, NUNC). After washing and blocking with 3% BSA for 1 hour, biotinylated monoclonal anti-VEGF antibody (100 µL/well of 6 nM biotinylated Avastin, or biotinylated Lucentis (100 µL/well of 2 nM)) was added, incubated 2 h and washed three times with PBS. NeutrAvidin, 170 pM, was added for 1 hour to select wells. The plate was washed three times with PBS, after which biotinylated phage, 60 pM (or 6 pM (10^8 phage/well) for the case of biotinylated Lucentis) was incubated in all wells for 1 hour. An

HRP/anti-M13 monoclonal conjugate (100 µL/well, 1:5000 diluted; GE Healthcare, 27-9421-01) was added, incubated for 1 h, washed three times with PBS and 100 µL 1-Step^{TM} Ultra TMB-ELISA Substrate (Thermo Scientific) were added to the wells. The reaction was stopped with 50 µL 2 M H_2SO_4 and absorbance was measured at 450 nm in a Tecan Infinite M200Pro microplate reader.

2.7.4 Comparison of antibodies for biotinylated phage/NeutrAvidin binding on ELISA plate

Two antibodies were compared for phage/NeutrAvidin binding to VEGF, biotinylated Lucentis (48 KDa) and biotinylated polyclonal anti-VEGF antibody (150 kDa), to determine which one is better suited for further experiments. VEGF in PBS, 2.6 nM, was incubated in wells for 2 h on a standard ELISA plate (Medisorb, 96-well, NUNC). The wells were washed and blocked with 3% BSA for 1 h. Biotinylated Lucentis, 100 µL/well of 2 nM (100 Lucentis molecules per later added phage /NeutrAvidin complex), 1 nM (50 Lucentis per 1 phage/NeutrAvidin), 0.2 nM (10 Lucentis per phage/NeutrAvidin), and 0.1 nM (5 Lucentis per phage/NeutrAvidin) and biotinylated anti-VEGF polyclonal antibody in the same molecule-to-molecule proportion (6 nM, 3 nM, 0.6 nM, and 0.3 nM) as Lucentis were added to select wells, incubated 2 h and washed three times with PBS. NeutrAvidin/phage complex (10^9 phage molecules per reaction), 170 pM, were added for 2 h to all wells containing the dilutions of the two biotinylated antibodies and no antibodies for control wells. The plate was washed

three times with PBS, and the captured phage was detected with an HRP/anti-M13 monoclonal conjugate as previously described in 2.7.3.

2.7.5 Evaluation of reaction buffers on ELISA plate

Using a similar approach as described in section 2.7.4, three different buffers were tested during the assay development. 50 mM Tris (60.1 g Trizma base in 400 ml H_2O, adjusted to pH 8.0 with approximately 20 mL concentrated HCl), PBS (0.95 g of Na_3PO4, 0.2 g KCl, 8.1 g NaCl in 1 L of H_2O, adjusted to pH 7.4 with NaOH), and PB (4.5 g of monobasic $Na_2H_2PO_4$ and 22.5 g of dibasic NaH_2PO_4 adjusted to pH 7.4 with NaOH) buffers were used as incubation buffers. In these experiments, the VEGF was diluted in Tris, PBS, and PB buffers prior to its incubation with the polyclonal anti-VEGF antibody. The incubation step was followed by three washes in the same buffer. The addition of biotinylated Lucentis was followed by the phage/NeutrAvidin complex, and then by an HRP-labeled anti-M13 antibody; incubations were undertaken in the same buffers as the original VEGF incubation.

2.8 PCR Assay Optimization

Real time PCR was used for visualizing the amplification of DNA fragments in real time. SYBR green dye was used for fluorescence measurements. The amount of fluorescent signal is directly correlated to the amount of product in reaction at that moment in time. The kit used is Brilliant III Ultra-Fast SYBR® Green PCR Master Mix (catalog number 600882, Agilent Technologies).

2.8.1 PCR Optimization

Before proceeding with assay development, it was crucial to determine the correlation between the Ct values generated by PCR and the concentration determined by tittering of infectious phage particles through titration. This was done by constructing a standard curve with a 10-fold phage dilution series. Here, a lower Ct value corresponded to the highest phage concentration.

2.8.2 Evaluation of phage stability

Standard curves were included with every experiment not only to determine the number of phage per reaction or evaluate the reproducibility of PCR, but also to monitor phage stability. For these experiments, 10-fold phage dilutions ($2*10^5$ to $2*10^9$) were made and refrigerated at 4°C. Those serial dilutions were used for three PCR experiments as described in Section 2.1.4 in the next ten days with five days between each PCR run.

2.8.3 Optimization of primer concentrations

It is well known that the primer concentrations used in PCR are most critical parameters and any variation will affect the slope of the standard curve. To avoid multiple freeze-thaw cycles, primers were diluted as required, aliquoted, and kept at -20°C. The experiments described in this section were performed using the same preparation of phage dilutions on two consecutive days. The forward and reverse primers were diluted to 5 µM and 3.3 µM concentrations (instead of 10 µM) and used with master mix prepared for PCR reaction, as described in section 2.5.

2.8.4 Avastin as the free VEGF-recognition antibody on polyclonal antibody particles

In order to determine the best magnetic particles assay for VEGF detection, a variety of options was examined. In this assay version, biotinylated Lucentis was substituted with biotinylated Avastin. VEGF was first captured onto anti-VEGF antibody-functionalized magnetic particles before biotinylated Avastin and pre-assembled NeutrAvidin/biotinylated phage were added for detection. 100 µL VEGF from 26 pM to 26 aM in PBS were mixed with magnetic particles (0.5 µg; ~$5*10^6$) functionalized with polyclonal anti-VEGF antibodies, and incubated on an orbital shaker for 2 h at 25°C. The NeutrAvidin/biotinylated phage (60 pM) and free biotinylated Avastin (6.7 nM) were added to the reaction simultaneously (final volume 100 µL). The reaction was allowed to incubate for 4 h at 25°C on an orbital shaker. After two washes with 0.3% Tween 20 in PBS to remove unbound phage and two washes with PBS, the particles were analyzed by PCR.

2.8.5 Polyclonal anti-VEGF antibody as the free VEGF-recognition antibody on Avastin-modified particles

In the second assay version, Avastin substituted the polyclonal anti-VEGF antibody on the particles. The bead surface modification was performed according to the protocol given above in Section 2.6.2.2 for the surface modification with polyclonal anti-VEGF antibodies. A biotinylated polyclonal anti-VEGF antibody was used to capture the phage/NeutrAvidin complex from one side and VEGF on particles modified with Avastin on the other. VEGF was first captured onto Avastin-functionalized magnetic particles before the

biotinylated polyclonal antibody and the pre-assembled phage/NeutrAvidin reagent were added for detection. 100 µL VEGF (26 pM to 26 aM) were mixed (in PBS and 20% bovine serum) with magnetic particles (0.5 µg; ~5*10^6) functionalized with Avastin, and incubated on an orbital shaker for 2 h at 25°C. The phage/NeutrAvidin (60 pM) and free biotinylated polyclonal anti-VEGF antibody (6.7 nM) were added to the reaction simultaneously (final volume 100 µL). The reaction was allowed to incubate for 4 h at 25°C on an orbital shaker. After two washes with 0.3% Tween 20 in PBS to remove unbound phage and two washes with PBS, the particles were analyzed by PCR.

2.8.6 Polyclonal anti-VEGF antibody as the free VEGF-recognition antibody on polyclonal anti-VEGF antibody-modified particles

VEGF was first captured onto polyclonal anti-VEGF antibody-functionalized magnetic particles before biotinylated polyclonal antibody and pre-assembled NeutrAvidin/biotinylated phage reagent were added for detection. 100 µL VEGF (26 pM to 26 aM) were mixed (in PBS and 20% bovine serum) with magnetic particles (0.5 µg; ~5*10^6) functionalized with polyclonal anti-VEGF antibody, and incubated on an orbital shaker for 2 h at 25°C. The NeutrAvidin/biotinylated phage (60 pM) and free biotinylated polyclonal anti-VEGF antibody (6.7 nM) were added to the reaction simultaneously (final volume 100 µL). The reaction was allowed to incubate for 4 h at 25°C on an orbital shaker. After two washes with 0.3% Tween 20 in PBS to remove unbound phage reagent and two washes with PBS, the particles were analyzed by PCR.

2.8.7 Optimization of particles surface coverage with anti-VEGF antibodies

To optimize the offered amount of antibody during functionalization, the number of magnetic particles per reaction and the number of the capture antibodies were adjusted. There were 10^9 particles and 10^{16} antibody molecules offered per reaction, which resulted in 10^7 antibodies offered/particle. The surface area of one antibody laying on its side (assuming cylindrical shape projected to the surface as a rectangle) is calculated using equation A = D*h = $15*10^{-17}$ m^2, where D and h are the diameter and height of an antibody ($3*10^{-9}$ and $5*10^{-9}$ m, respectively). The surface are of a 1-mm bead is calculated using the surface area of a sphere: $A = 4\pi r^2 = 3.14 * 10^{-12}$ m^2, where the radius of a bead is equal to $0.5*10^{-6}$ m. The number of antibodies offered is estimated to (10^7 * 15 * 10^{-17}) / (3.14 * 10^{-12}) = 4.8 monolayers.

In an attempt to optimize the performance of the capture particles, antibodies were also offered at lower concentrations during particle functionalization. One third and one tenth of the original 10^{14} antibodies per reaction (1.6 and 0.48 monolayers respectively) were added and the original protocol for functionalization was followed as described in Section 2.6.2.1.

2.8.8 Avastin-modified 250 nm magnetic particles

Smaller particles of diameter 250 nm were also explored as capture particles. The assay approach was performed as explained in Section 2.1.2. In short, 250 nm magnetic particles functionalized with Avastin (as suggested by manufacturer) were incubated with 100 µL of VEGF diluted from 2.6 nM to 2.6 pM in PBS for 2 h at 25°C on an orbital shaker, washed 3 times with PBS and

blocked with 3% BSA. After 3 PBS washes, the free biotinylated polyclonal anti-VEGF antibody and NeutrAvidin/phage complex were mixed together and incubated for 4 h at 25°C on an orbital shaker. After two washes with 0.3% Tween 20 in PBS to remove unbound phage reagent and two washes with PBS, the particles were analyzed by PCR.

2.9 Results and Discussion

2.9.1 Biotinylation of Phage

The results of phage biotinylation are presented in **Figure 9.** There is some degree of biotinylation to AviTag phage during growth, so the OD signal from non-enzymatically biotinylated phage is not a zero. However, phage biotinylated with biotin ligase produced a higher signal than the original AviTag phage in any dilution. The highest OD measurement corresponded to the highest biotinylated phage concentration, while the no-phage control signal was similar to the background.

2.9.2 Biotinylation of Antibodies

Three different types of antibodies were biotinylated as described earlier in Section 2.5.1 and the average number of biotin molecules per one antibody molecule was calculated. The full-length polyclonal anti-VEGF antibody has the highest degree of biotinylation (5.7 biotin molecules per one antibody), while Avastin, the monoclonal antibody (also the full length), has much less biotin molecules after biotinylation (1.4 biotins per antibody). This number is similar to the number of biotins on Lucentis (1.5 per antibody), the Fab-fragment derived

from Avastin. The number of biotin molecules on non-biotinylated Lucentis was zero, which implies that there are no biotin molecules originally in the Lucentis. Other non-biotinylated controls (of Avastin and polyclonal anti-VEGF antibody) were not performed.

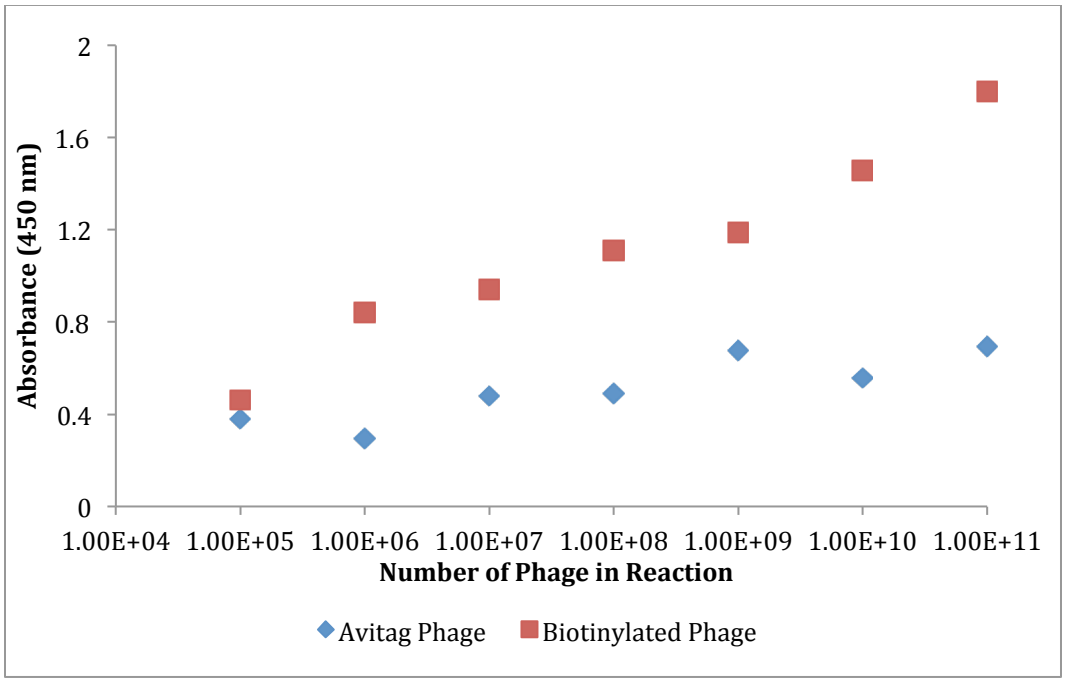

Figure 9: **ELISA result of phage biotinylation.** *The highest absorbance signal corresponds to the highest phage concentration. The reference for the degree of biotinylation is the Avitag phage, which is, originally, 40% biotinylated. Assuming that the majority of the phage binds to the streptavidin surface, the signal for biotinylated phage should be approximately 60% higher than for the Avitag phage, which is shown on the graph.*

2.9.3 Lucentis binding assay

Biotinylated and non-biotinylated Lucentis were adsorbed on a Streptavidin plate, washed, and blocked with 3% BSA. The HRP-labeled Streptavidin was used as a read-out signal for colorimetric ELISA. As a result,

Lucentis in combination with HRP-labeled Streptavidin were determined to be suitable for this assay: Lucentis modified with biotin showed a much higher binding than non-biotinylated Lucentis. As seen from **Figure 10**, the HRP-labeled Streptavidin showed a low background (0.1 for original Lucentis and 0.36 for biotinylated Lucentis) for lowest concentration of Lucentis (20 fM). The background for zero Lucentis in both cases was at OD signal of 0.1.

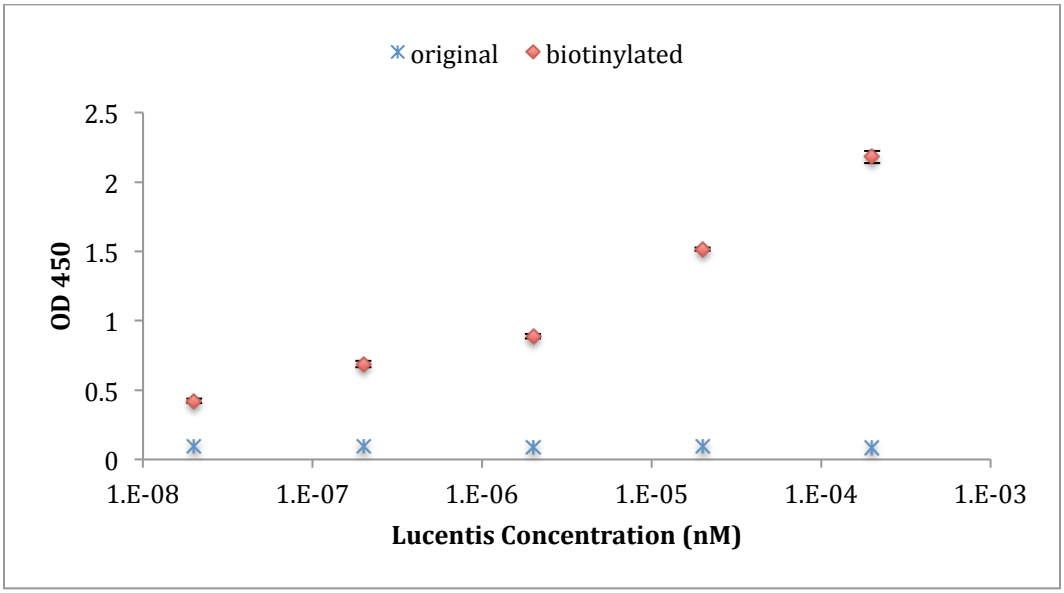

Figure 10: Lucentis binding assay. *Detection of biotinylated and non-biotinylated Lucentis with streptavidin-HRP on ELISA plate, (n=2).*

2.9.4 Phage PCR amplification efficiency

Since amplification of phage nucleic acids is the output of the assay, we first prepared standard curves for the accurate correlation of phage titering to PCR signal. The phage stock was serially diluted 10 to 10^{11}-fold and the number of phage in each dilution was determined by the classic agar overlay technique [16]. Phage then served as template in real-time PCR with primers specific for

AviTag phage. As shown in **Figure 11**, phage amplify with an average reaction efficiency of 109.2% ± 6.64 (slope of standard curve = 3.1 ± 0.15), based on instrument-generated results. We determined the linear range of detection for phage by real-time PCR to extend from 10^5 to 10^{10} phage/mL, or $5*10^2$ to $5*10^8$ phage particles per reaction by correlating the real-time PCR signal to number of phage per reaction pre-determined microbiologically (**Figure 11**).

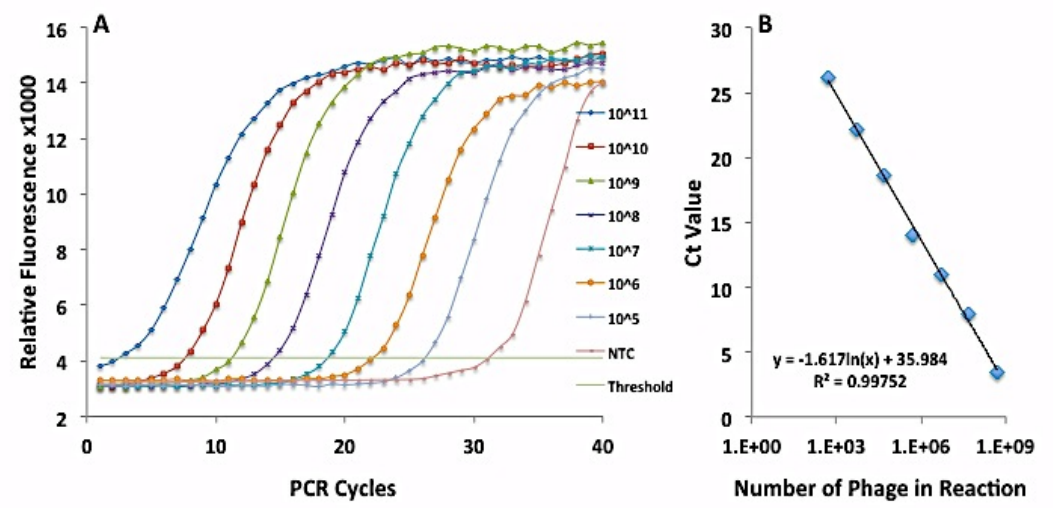

Figure 11: **Detection of immuno-phage using real-time PCR.** *(A) Amplification plots of 10-fold serial dilutions of phage ($5*10^2$-$5*10^8$ phage/reaction) by real-time PCR using primers targeting the AviTag-encoding DNA sequence. (B). Correlation of real-time PCR Ct values and phage number (phage concentration was based on phage titers estimated through an agar overlay).*

2.9.5 Phage-mediated VEGF immunoassay with Avastin on ELISA plate

As shown on the graph (**Figure 12**), skipping one or more reagents at a time proved that there was no or low cross-reactivity of any individual reagent with subsequent layers, biotinylated phage, or HRP-labeled antibody. The highest signal corresponded to layers of all reagents without omission, while in

the case when one or more of the reagents were omitted, the signal decreased significantly.

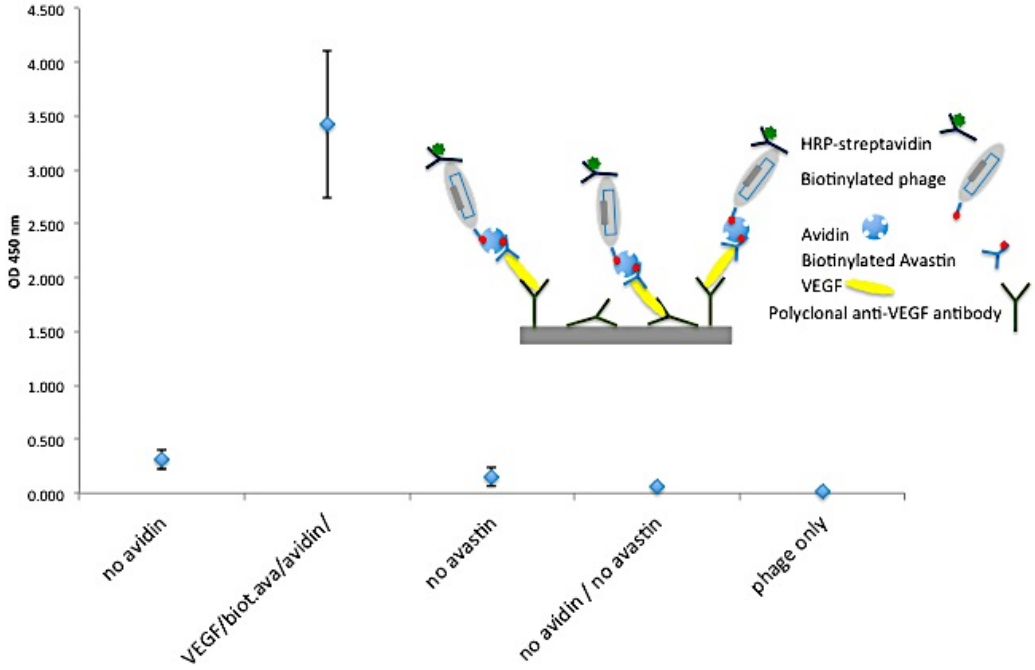

Figure 12: **VEGF detection by ELISA using biotinylated Avastin.** *The assay followed "one-at-a-time" format, with one of the reagents omitted from the layers (n=4).*

2.9.6 Comparison of antibodies for biotinylated phage/NeutrAvidin binding

To determine the optimum antibody for phage/NeutrAvidin binding to VEGF two options were explored: the binding of biotinylated Lucentis (Lucentis, 48 kDa) and the binding of biotinylated polyclonal anti-VEGF antibody (150 kDa). The biotinylated Avastin was not included as an option because of assay sensitivity. Unfortunately, the experiments with Avastin, as a detection antibody, only resulted in "yes" or "no" control for pathogen detection. The assay was not sensitive enough to distinguish among various VEGF

concentrations in solution when compared with biotinylated Lucentis. The biotinylated Lucentis has a very strong affinity towards VEGF, while having only 1-1.5 biotins per antibody molecule. On the other hand, biotinylated polyclonal antibody can be modified with as much as 5 biotin molecules per antibody molecule on average, providing a better chance for phage/NeutrAvidin to attach.

The phage concentration for these experiments was held constant, at 10^9 phage molecules per reaction; the VEGF concentration was constant at 2.6 nM The number of antibodies put in reaction was varied from 100, 50, 10, 5, to zero antibodies per phage/NeutrAvidin molecule. Biotinylated Lucentis showed a better VEGF binding than polyclonal anti-VEGF antibody. The background for no-antibody control was at a level of 0.25-0.27. The highest OD measurement of biotinylated Lucentis was equal to 1.48, while for biotinylated polyclonal anti-VEGF, the highest OD signal corresponded to 0.97.

From this experiment it was concluded that biotinylated Lucentis can capture VEGF from solution better than polyclonal anti-VEGF antibody (**Figure 13**); also, it was determined that the highest ratio of 100 molecules of biotinylated Lucentis per one phage/NeutrAvidin molecule would provide a more efficient binding to VEGF. Higher ratio of 1000:1 was not assayed because of limited available amounts of the precious Lucentis. On the other hand, when comparing this assay to the one with biotinylated anti-VEGF polyclonal antibody, one can see that at higher concentrations of phage/NeutrAvidin

molecules per one antibody molecule, the assay with polyclonal antibody came to a plateau, while assay with biotinylated Lucentis still exhibited higher binding.

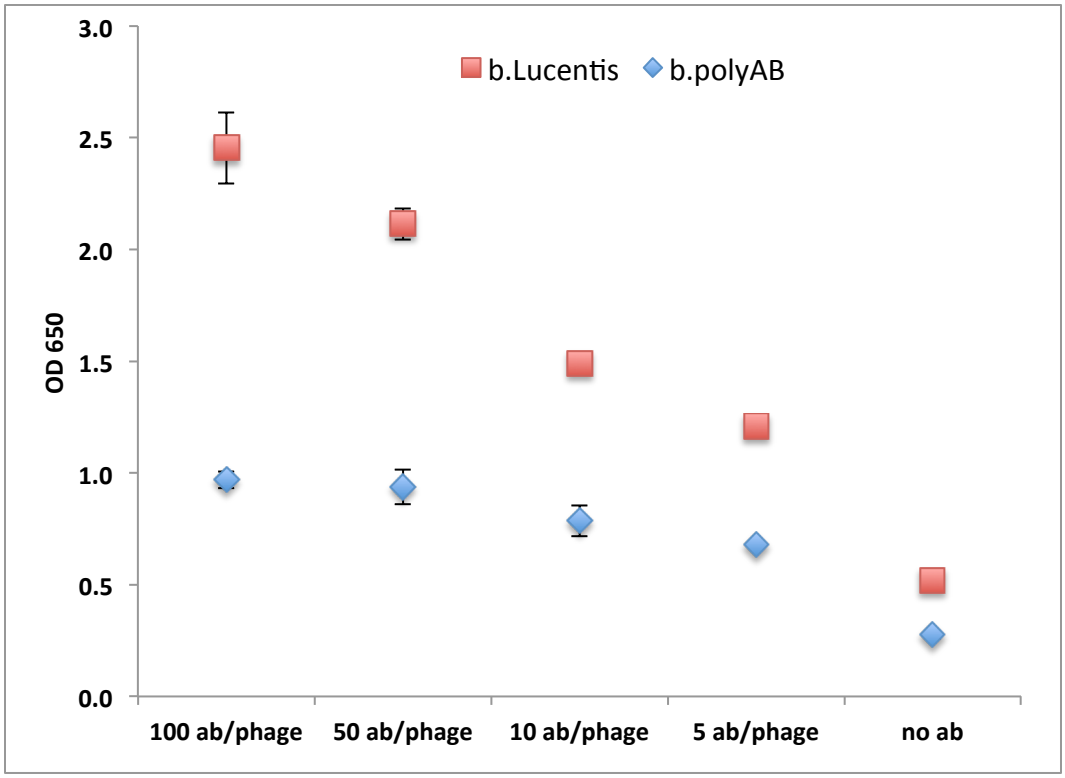

Figure 13: **ELISA result for comparison of biotinylated Lucentis and biotinylated polyclonal anti-VEGF antibodies for VEGF binding.** *Polyclonal anti-VEGF antibody was adsorbed on ELISA plate, followed by addition of VEGF, biotinylated Lucentis (or biotinylated polyclonal antibody), and phage/NeutrAvidin complex. (n=2).*

2.9.7 Phage-mediated VEGF immunoassay with Lucentis on ELISA plate

Based on **Figure 14**, the Lucentis-based detection of different concentrations of VEGF showed results similar to that of Lucentis in the approach where one of the layers' reagents were omitted from the incubation steps. The assay showed reasonable sensitivity for ELISA, with an LOD at approximately 26 pM. The non-specific binding observed was minimal.

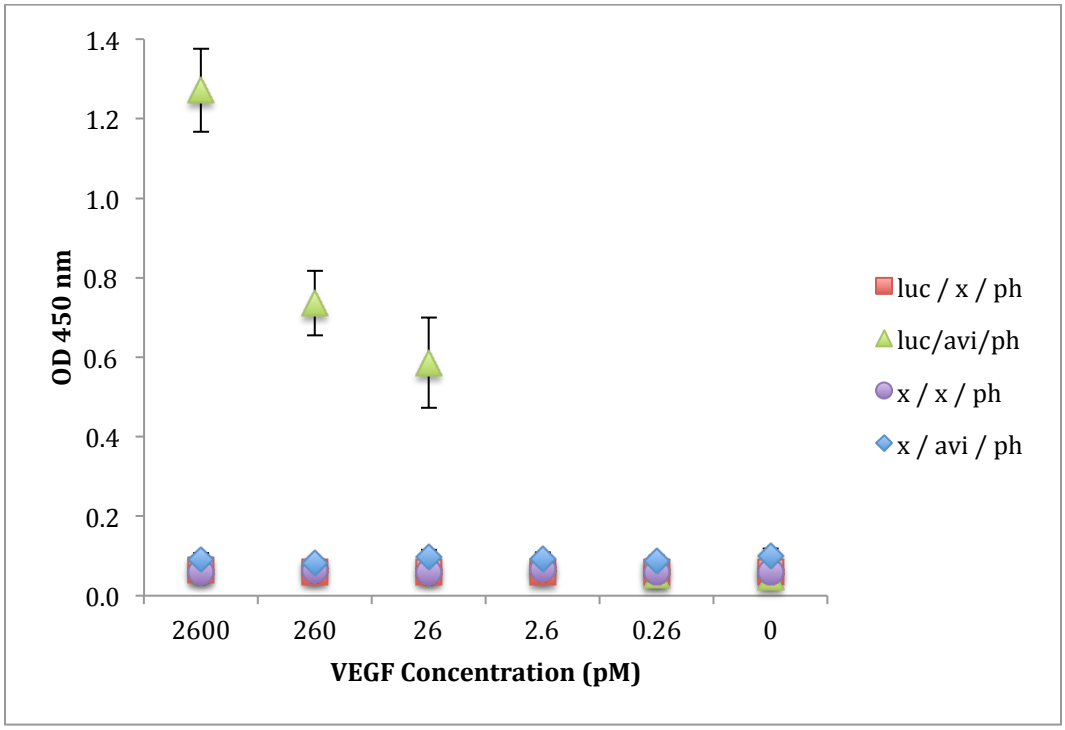

Figure 14: **ELISA of VEGF detection using biotinylated Lucentis.** *The assay followed "one-at-a-time" format, with one of the reagents (shown with an* x*) omitted from the layers (n=2).*

2.9.8 Phage-mediated VEGF immunoassay with Lucentis using streptavidin-HRP on ELISA plate

As shown in **Figure 15**, the limit of detection of this assay was 6.3 pM, which was in agreement with previously published results for VEGF ELISA assays [65-67]. Streptavidin-HRP was used instead of HRP-labeled antibody for this detection assay. Thus, the antibodies were proven to be of sufficiently high affinity for the demonstration of the novel assay.

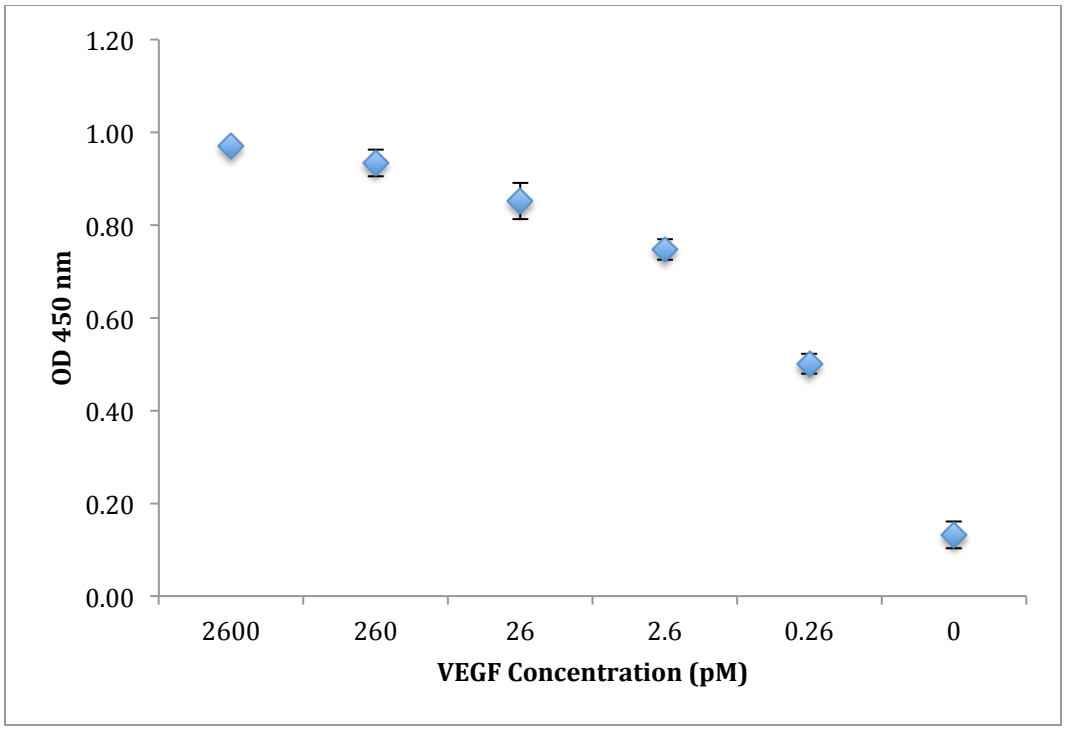

Figure 15: **ELISA for VEGF detection with biotinylated Lucentis using streptavidin HRP.** *VEGF detection in PBS following "one-at-a-time" format. Polyclonal anti-VEGF antibody was incubated in wells, followed by addition of VEGF dilutions and Lucentis. HRP-labeled streptavidin was used for detection (n=2).*

The blocking step was usually performed to "fill in" the empty space among the VEGF molecules on the ELISA plate. While this might not be necessary when reagents are present in high concentrations and non-specific binding is not a critical issue, the blocking step in any immuno-phage assay is crucial when the concentration of one of the reagents is in extremely low ranges.

When using smaller number of molecules, more empty space becomes available on the plate, giving rise to more non-specific binding of other reagents during later steps. The assay was performed as described in Section 3.2 and the phage construct was prepared as described in section 2.6.3, the "Antibody-phage

format." As seen in **Figure 16**, blocking with 3% BLOTTO in PBS, resolved the 2.6 nM of VEGF, while for blocking with 3% BSA, the limit of detection was close to 26 pM.

The assay with 3% BLOTTO blocking showed a lower OD signal than with 3% BSA blocking. The reason for this might be that BLOTTO, being complex dry skim milk, is more effective in blocking a protein itself (i.e., VEGF), while BSA is more effective in filling spaces in between the VEGF molecules.

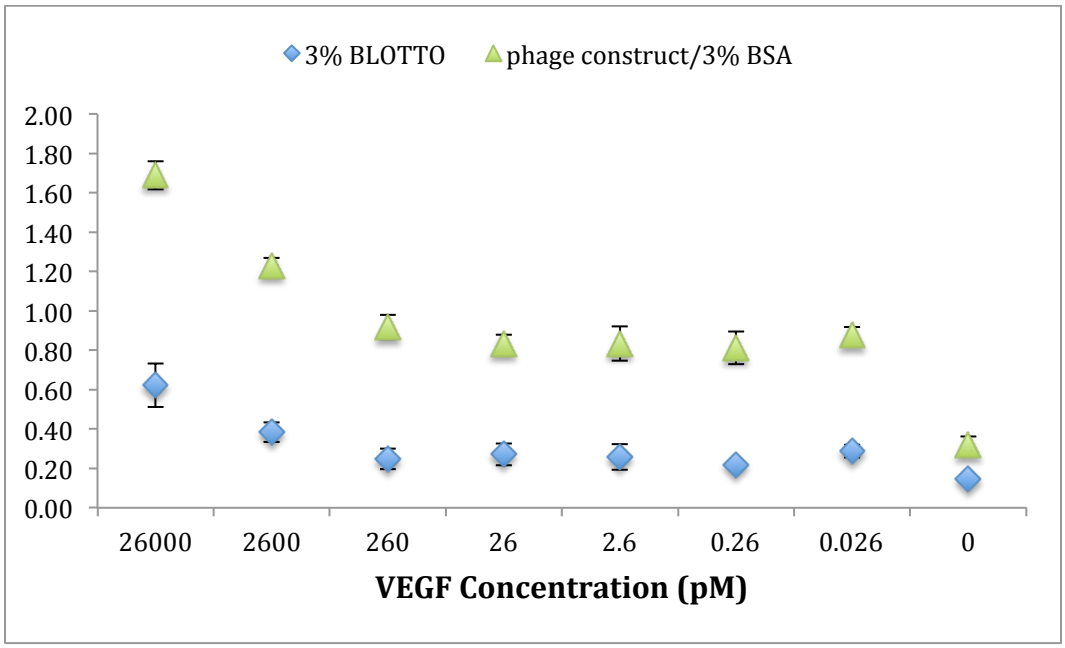

Figure 16: **ELISA result of blocking reagents** *(3% BLOTTO and 3% BSA in 1xPBS). VEGF detection followed "antibody-phage" format, where pre-assembled phage/Neutravidin/antibody particles were used to detect VEGF from solution.*

2.9.9 Evaluation of reaction buffers

Three different buffers were used to determine whether the pH or buffer composition/concentration were limiting factors for the assay development. 50

mM Tris at pH 8, 150 mM PBS at pH 7.4, and 100 mM PB at pH 7.4 were used as incubation buffers. As can be seen in **Figure 17**, Tris buffer showed a lower signal than PBS or PB. The two other buffers, PBS and PB, showed similar binding of the reagents in assay. PBS was chosen to proceed with since it is a standard assay buffer widely used.

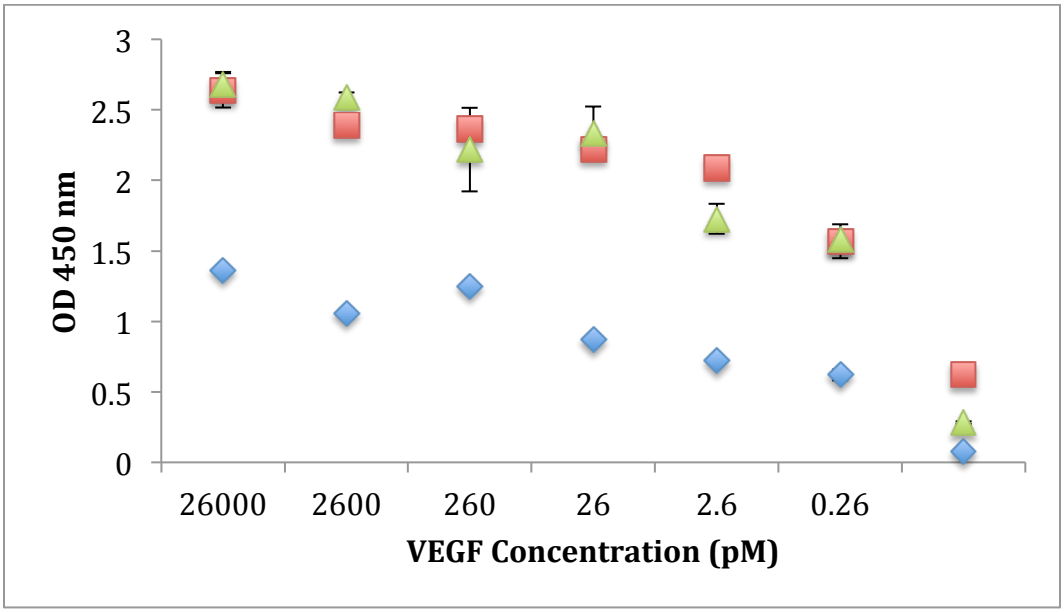

Figure 17: **Evaluation of different incubation buffers** *50 mM Tris at pH 8 (blue diamonds), 150 mM PBS at pH 7.4 (red squares), and 100 mM PB at pH 7.4(green triangles) were used as incubation buffers.*

2.9.10 Evaluation of PCR standard curves

The standard curve usually was a straight line with an R^2 value higher than 0.98. The average difference between the individual Ct values for each of the 10-fold serial dilutions of phage corresponded to 3 - 3.5 Ct values, resulting in the range of approximately 30 Ct values for phage concentrations from $2.5*10^3$ to $2.5*10^{10}$ as shown in **Figure 18**.

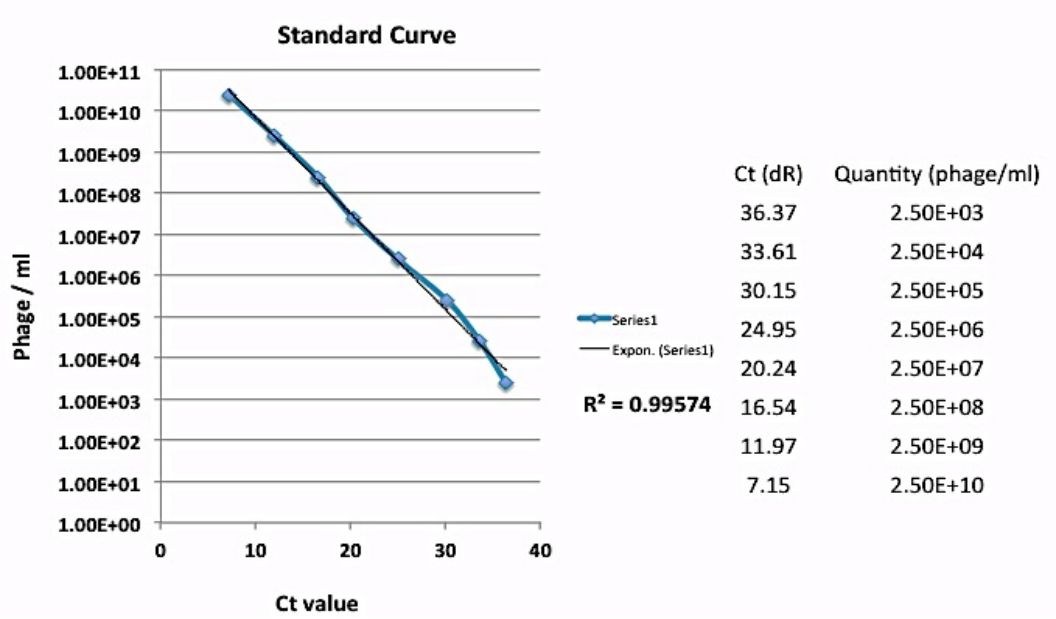

Figure 18: PCR standard curve and Ct-to-phage number correlation.

2.9.11 Evaluation of primer concentrations and reproducibility of standard curves

As one can see, the dilution of primer to a 5 µM and 3.3 µM (from the original concentration of 10 µM) affected the Ct values, i.e., the 1/2 –diluted primers (5 µM) had higher Ct values than 2/3 -diluted primers (3.3 µM) for the same phage dilutions, as shown in **Figure 19**. Two experiments were performed in two consecutive days to avoid any issues of possible phage degradation. Both experiments confirmed that the same primer concentration would reproduce the result for the same phage dilution. Also, phage dilutions were stable within 2 days of their preparation (**Figure 20**), indicating that antibody-phage constructs do not have to be freshly made just before the experiments and may be stored for at least a short time.

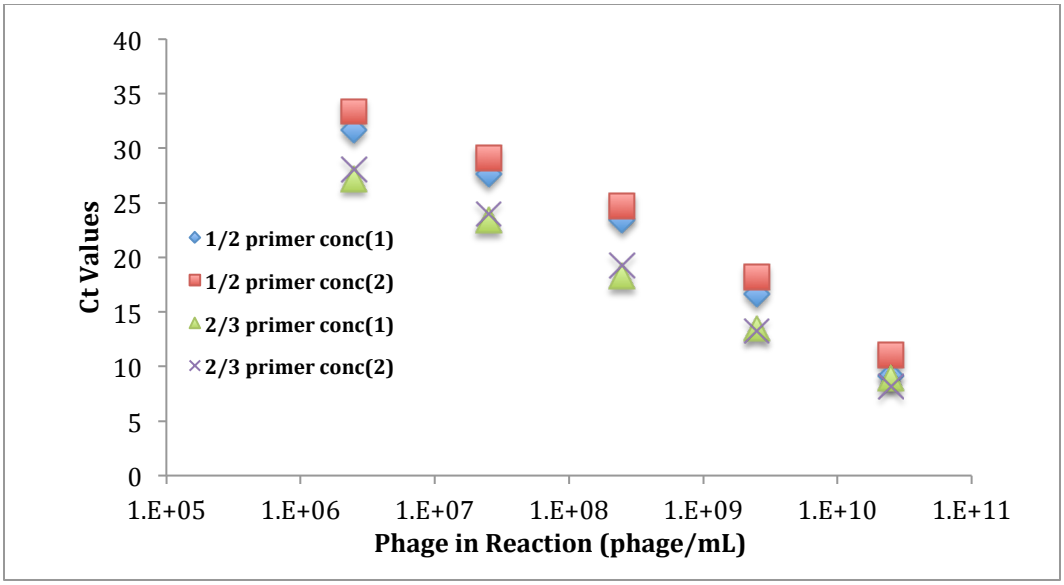

Figure 19: **Primer concentration optimization.** *Primers at 2 different concentrations used for the amplification of the same phage dilutions at different days.*

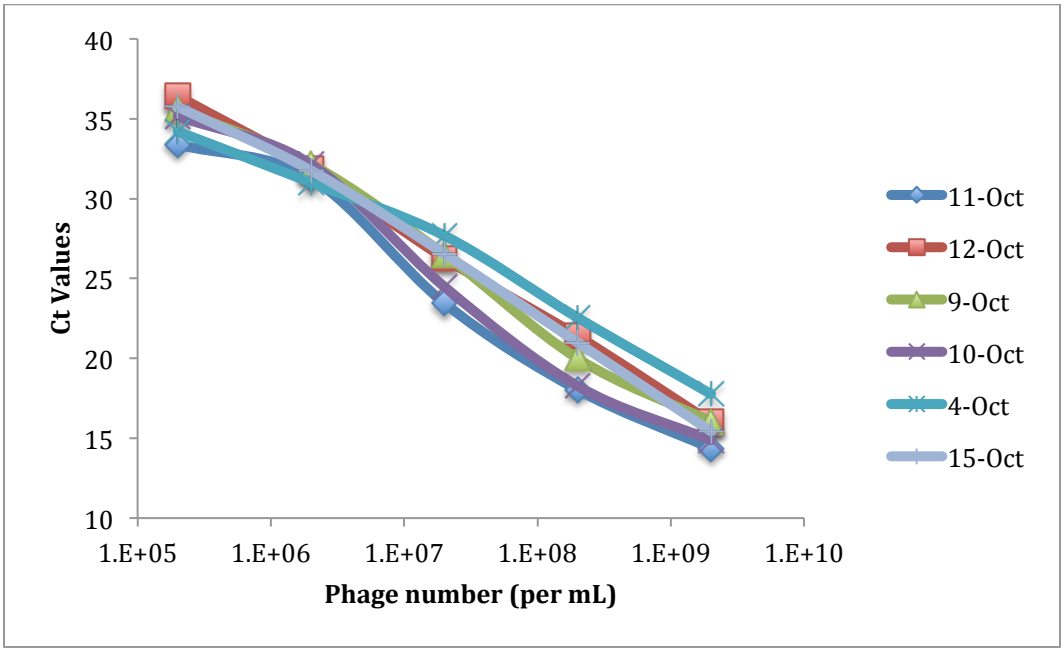

Figure 20: **Reproducibility of standard curves.** *Amplification of the same phage dilutions at different days.*

2.9.12 Evaluation of phage stability

When a series of phage dilutions were analysed by PCR in consequtive days, it was observed that the samples of the highest concentration showed similar Ct values whereas more dilute samples showed deviation from 3 to 5 Ct values (**Figure 21**). It was concluded that biotinylated phage in low concentrations was either not stable when stored for longer than one week or was sticking to the tube's walls. As a result, instead of blocking the tubes with 3% BSA, the same phage dilutions for standard curves were used for one week only, after which they were discarded and new phage dilutions were made (Figure 21). This was also observed later with phage constructs, which were also found not stable for more than 5-7 days.

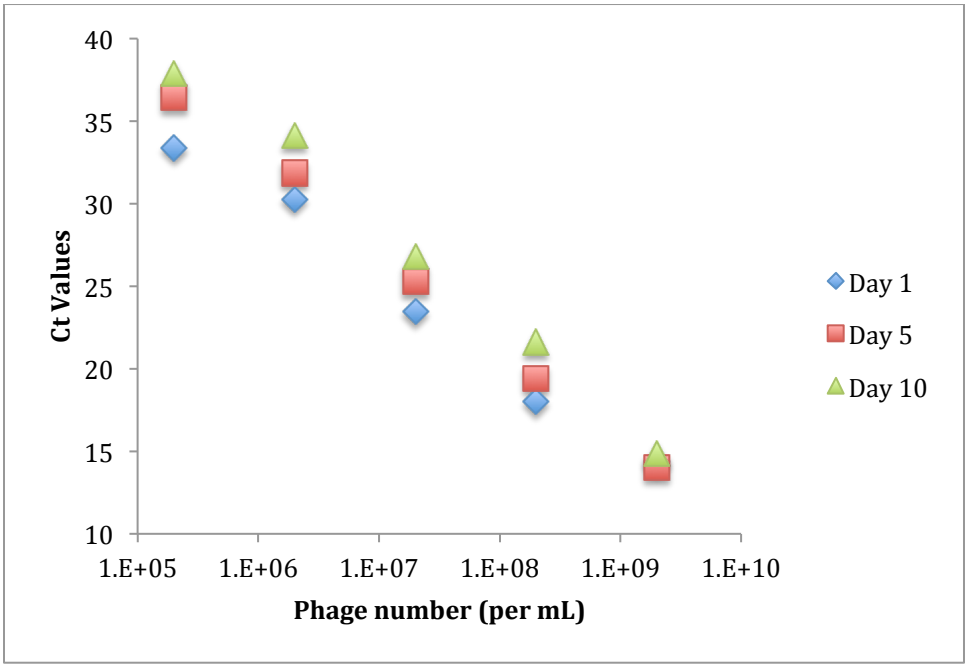

Figure 21: **Comparison of PCR standard curves for same phage dilutions.** *Phage stability issues. A series of phage dilutions analysed by PCR showed similar Ct values for the highest concentration and deviation from 3 to 5 Ct values for lower concentrations.*

2.9.13 Avastin-modified particles with polyclonal anti-VEGF free biotinylated antibody in "avidin-phage" format

Avastin was tested instead of polyclonal anti-VEGF antibody on the 250 nm magnetic particles. The particles surface modification was performed according to the protocol as given above for surface modification with polyclonal anti-VEGF antibody. Biotinylated polyclonal anti-VEGF antibody, in turn, was used to capture biotinylated phage/NeutrAvidin complex from one side and VEGF on particles modified with Avastin on the other. Although an expected trend was observed between the VEGF concentration and the Ct values, the correlation did not have high enough R^2 value to be considered as promising. Also, the size of the error bars and the very similar Ct values of the last two VEGF concentrations did not make the assay sensitive enough for further considerations, as in **Figure 22**.

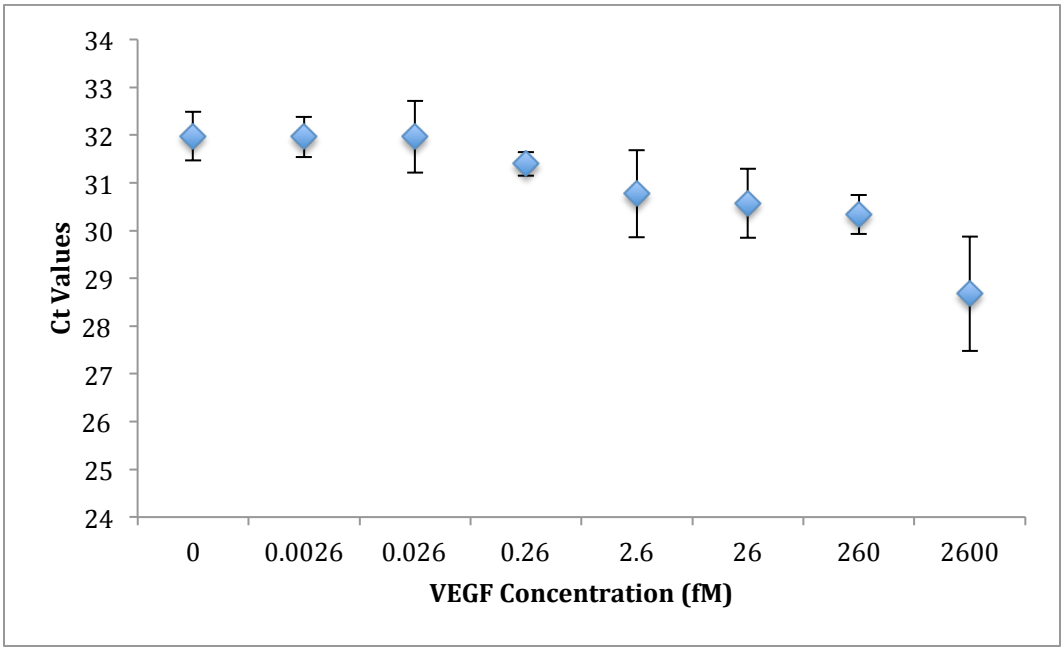

Figure 22: **VEGF detection in the "avidin-phage" format with biotinylated polyclonal antibody (1).** *VEGF detection in PBS using the pre-assembled NeutrAvidin-phage complex with free biotinylated polyclonal antibody.*

2.9.14 Polyclonal anti-VEGF antibody as VEGF-recognition antibody on polyclonal anti-VEGF antibody-modified particles

The third approach involved the use of polyclonal anti-VEGF antibody both as antibody for bead surface modification and as the free biotinylated antibody for VEGF recognition **(Figure 23)**. In this assay, the particles surface modification was performed according to the same protocol (for particle surface modification with polyclonal anti-VEGF antibody). The antibody on particles was not biotinylated.

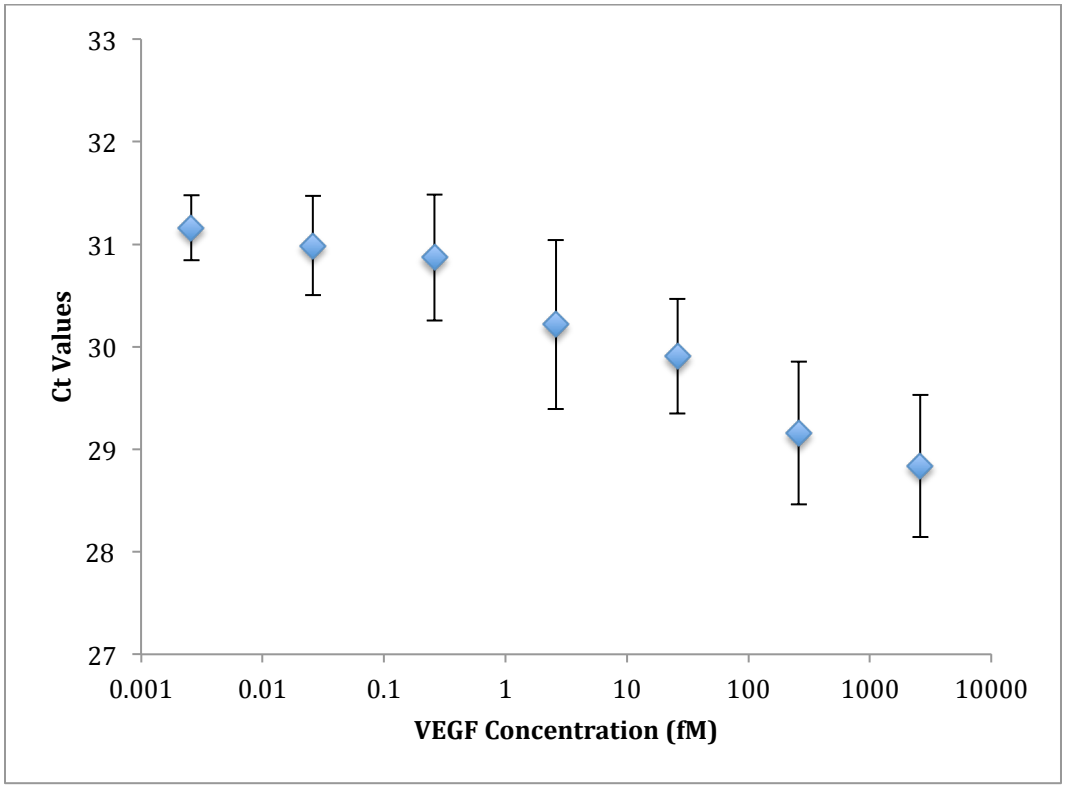

Figure 23: **VEGF detection in the "avidin-phage" format with biotinylated polyclonal antibody.** *VEGF detection in PBS using the pre-assembled NeutrAvidin-phage complex with polyclonal anti-VEGF antibody both as*

antibody on the capture particles and as the free biotinylated antibody for VEGF recognition.

The biotinylated polyclonal anti-VEGF antibody was used to capture biotinylated phage/NeutrAvidin complex from one side and VEGF on particles modified with polyclonal anti-VEGF antibody on the other. The experimental set-up was the same as used in previous sections. As can be seen from **Figure 23**, the experiment in PBS showed a better correlation between VEGF concentration and their corresponding Ct values then for the other two approaches. However, the calculations of the assay detection limit averaged at 11 pM, which was decided not be sensitive enough for a reasonable PCR assay.

2.9.15 Antibody coverage for particles functionalization

Antibody amounts were optimized for particles surface modification [68]. An experiment of "antibody-phage" format was performed as described in Section 2.1.3. Unfortunately, the results did not improve for lower antibody bead coverage and there was no correlation between VEGF concentration and Ct values. **Figure 24** shows the results of VEGF assay using the original amount of antibody, as given in protocol in Section 2.6.2.1. It was decided to proceed with the original amount of antibodies for surface functionalization, as explained in Section 2.3.1.

2.9.16 Avastin-modified 250 nm particles

Carboxylated 250-nm magnetic particles were modified with Avastin (the monoclonal anti-VEGF antibody) instead of a polyclonal anti-VEGF antibody, as described in Section 2.5.2.2. As one can see from **Figure 25**, the change of

antibody on particles did not yield any improvement to the assay. Although the Ct values and the VEGF concentrations did follow the required trend, the delta Ct value was less than 2, the error bars were too large to distinguish among the VEGF concentrations, and the R^2 value of the experimental curve was 0.88. The limit of detection was calculated to be equal to 13 pM VEGF concentration. Also, the assumption that only one phage binds on one magnetic bead did not hold, since the number of the 250-nm particles was 10-fold higher than the number of the 1 µm particles per assay, and the number of phage bound to particles surface did not increase as a result of increase in particles number (Figure 25).

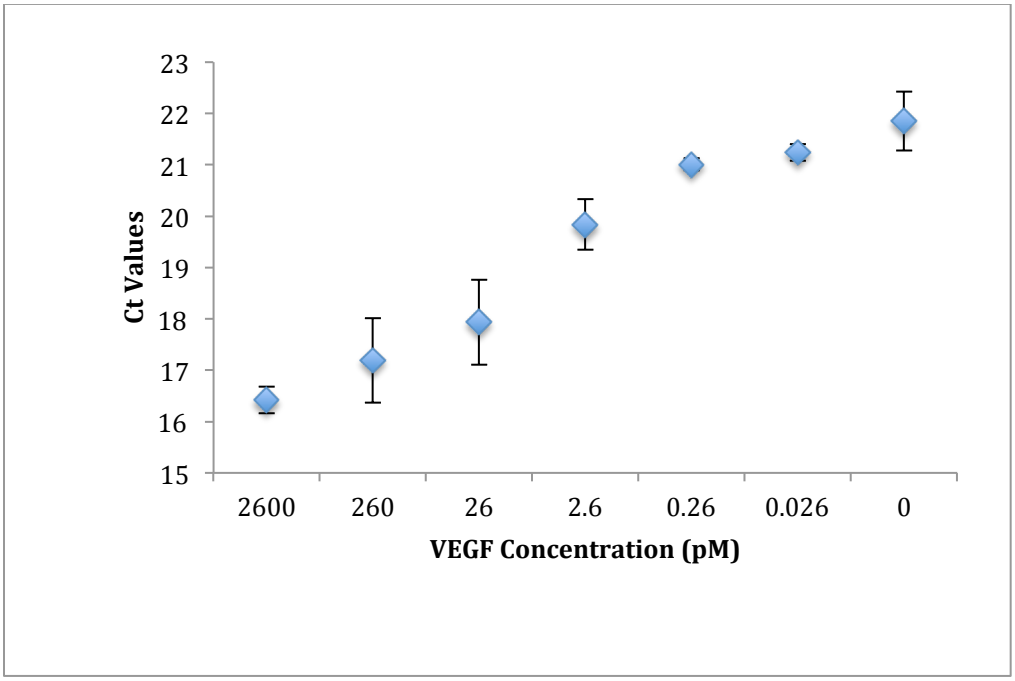

Figure 24: **Optimization of bead surface coverage.** *Original amount of antibody were offered for surface functionalization of 1µm particles, the protocol for antibody-phage format was followed and the results were analyzed in PCR.*

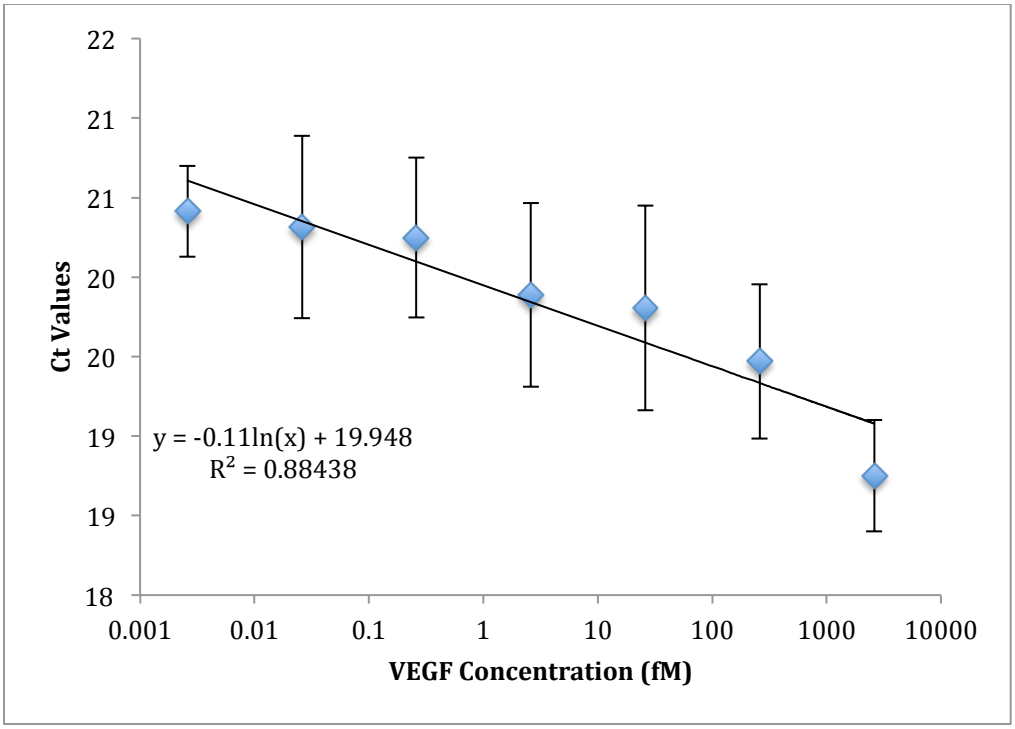

Figure 25: **VEGF assay on Avastin-modified 250 nm magnetic particles.** *VEGF detection in the "avidin-phage" format with biotinylated polyclonal antibody as free antibody in solution and Avastin as antibody for particles surface functionalization.*

2.9.17 ELISA with Streptavidin HRP

Polyclonal anti-VEGF antibody was adsorbed on the bottom of a 96-well microtiter plate and decreasing concentrations of VEGF (260 pM to 2.6 fM in buffer, along with a no-VEGF control) were added to each well. The protocol was followed as explained in Section 2.6.5. As shown in **Figure 26**, the limit of detection of this assay was 260 fM, which is in agreement with previously published results for VEGF ELISA assays [65-67]. The LOD of the assay was determined by subtracting three standard deviations from the mean Ct value of the no-VEGF control and calculate the analyte concentration from the Ct vs. VEGF concentration curve.

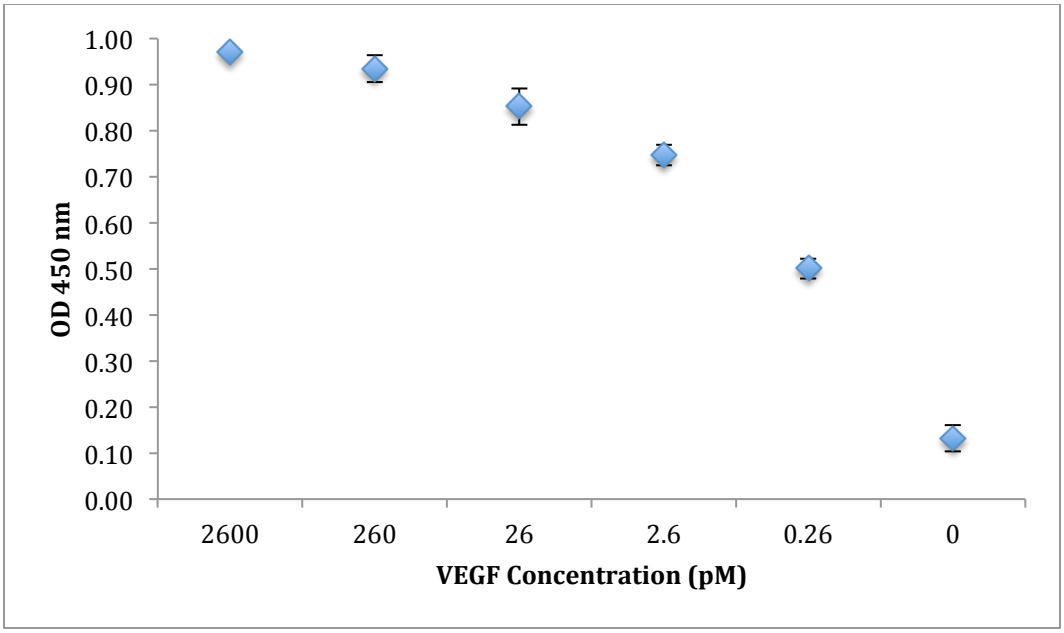

Figure 26: **ELISA for VEGF detection with biotinylated Lucentis using Streptavidin HRP,** *(n=2).*

2.9.18 Phage immuno-PCR – "One-at-a-time" format

Initially, a stepwise process was followed, in which each assay component is added to the reaction individually, and various wash steps remove excess components after each addition. While time-consuming, this "one-at-a-time" approach allowed for the careful evaluation and optimization of each step of the assay, and yielded a well-defined preparation of immuno-phage particles for our initial experiments. We were able thus able to optimize incubation times, reagent concentrations, and washing conditions. Specifically, we found that any concentration of phage between 6 - 600 pM produced similar results. Likewise, we determined experimentally that 0.3% Tween 20 added to the wash buffer removed non-specifically bound phage, but did not affect phage specifically bound on the magnetic particles (data not shown).

As shown in **Figure 27**, VEGF was spiked into buffer at concentrations ranging from 2.6 nM to 2.6 fM and the limit of detection (LOD) was determined to be approximately 3 fM. The LOD of the assay was determined by subtracting three standard deviations from the mean Ct value of the no-VEGF control and inferring the analyte concentration from the Ct *vs.* VEGF concentration curve. This concentration is approximately 100-fold lower than the LOD established for the ELISA assay (using the same antibody pair), emphasizing the improved sensitivity gained through the use of real-time PCR as the reporter. The error bars were calculated based on propagation error, where the standard deviation on the no-VEGF control is added to the standard deviation of the individual data points of each VEGF dilution.

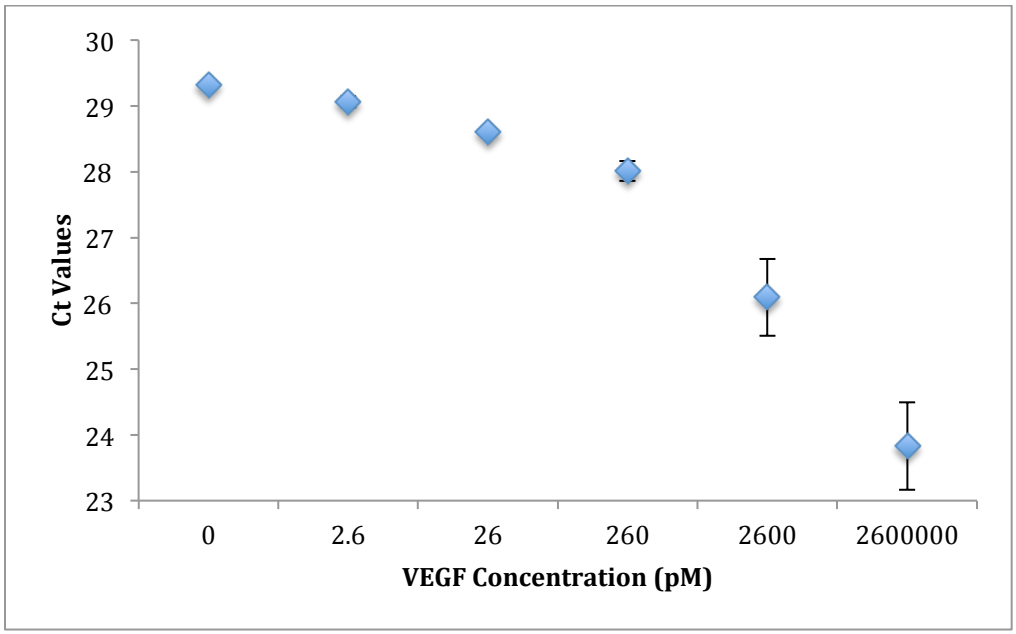

Figure 27: **The One-at-a-time format.** *Reagents are added one by one to 1 μm magnetic particles modified with polyclonal anti-VEGF antibody (VEGF, biotinylated Lucentis, Neutravidin, biotinylated phage; incubation of each layer is followed by 3 washes in PBS), n=3.*

2.9.19 Two-step Assay Development

After the "one-at-a-time" approach allowed validation of the superior sensitivity of immuno-detection using functionalized AviTag phage, we further explored the use of modified phage-based immuno-reagents in two simpler protocols (**Figure 28**). In the "avidin-phage" approach, VEGF is first captured onto antibody-functionalized magnetic particles before the second biotinylated antibody and pre-assembled NeutrAvidin/biotinylated phage reagent are added for detection. This approach required fewer wash steps and was less time-consuming and still yielded a lower LOD of 0.55 fM (Figure 25), approximately 500-fold lower than that of the ELISA.

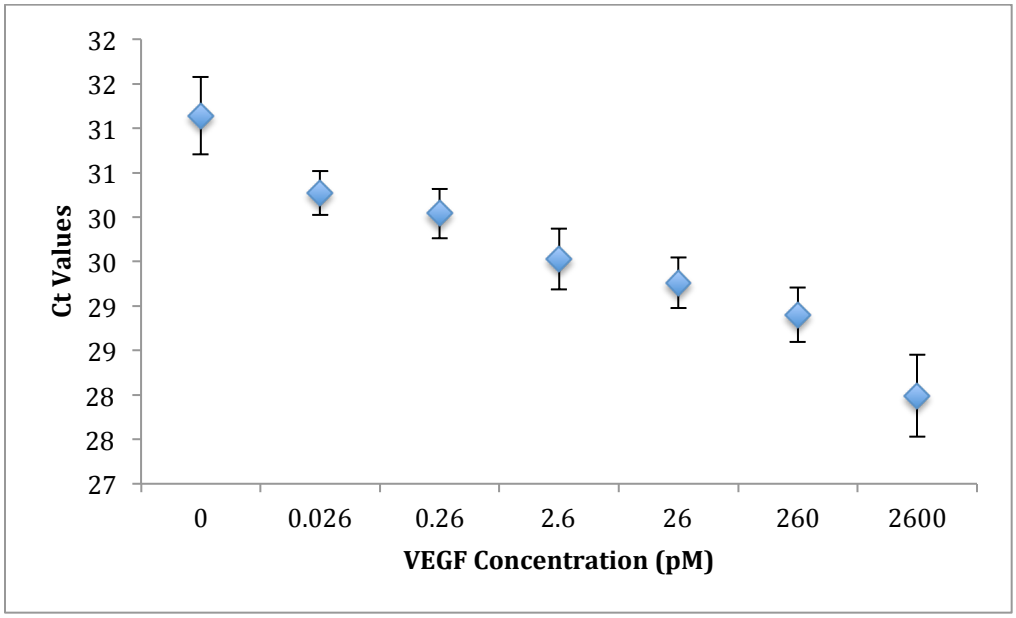

Figure 28: **VEGF detection in the "avidin-phage" format.** *VEGF detection in PBS using the pre-assembled immuno-phage/Neutravidin construct ("antibody-phage" format); n=6, error bars = ±1 SD, NTC >35.*

2.9.20 One-step Assay Development

A final variation of the assay protocol uses a pre-assembled antibody/NeutrAvidin/biotinylated "antibody-phage" construct. In this approach,

antibody-functionalized magnetic capture particles are added to the target solution, and, after a single wash step, the integrated immuno-phage reagent is added for detection. Figure 13 demonstrates that the LOD obtained with this approach is 64 fM, 4 times lower than that of ELISA, but with a much simpler and rapid protocol (**Figure 29**), also, taking into account the 2 h assay time, comparing to more than 8 h for "one-at-a-time" format assay.

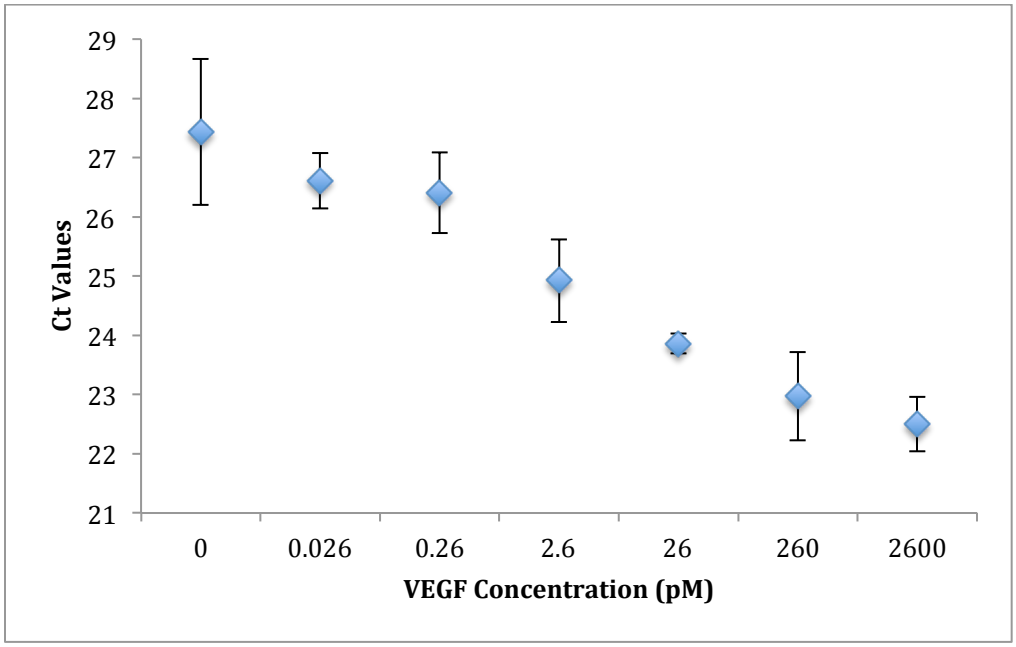

Figure 29: "Antibody-phage" assay in PBS. *VEGF detection in PBS using the pre-assembled antibody-phage construct; n=6, error bars = ±1 SD, NTC >35*.

2.9.21 Assay reproducibility

To check inter and intra-assay reproducibility, a range of 7 different concentrations of VEGF and a no-VEGF negative control were assayed in six replicates on each of 5 days (i.e. 5 independent experiments) using the efficient "antibody-phage" format. All experiments were performed in PBS. For every

experiment, a new batch of immuno-phage particles was prepared the day before the assay was performed from pre-made stocks of bacteriophage and Lucentis as described earlier. The between-day CV on the positive ("positive") and no-VEGF control ("negative") samples tested in 6 replicates are presented in **Table 1**. The high degree of agreement between the determined LOD values each day highlights the fact that the assay is robust and reproducible (**Figure 30**).

Table 1. VEGF assay in PBS: The coefficient of variation (COV) and limit of detection calculation (LOD). *VEGF was assayed in PBS in 6 replicates on five different days (total sample number for each concentration, n=30). The coefficient of variation (COV) for each day was calculated as: COV%= 100*SD/mean. The LOD was determined by subtracting three standard deviations from the mean Ct value of the no-VEGF control (6 replicates) and calculate the concentration from the corresponding standard curve.*

	Coefficient of Variation of Ct (%) = SD/MEAN*100		LOD
	Positive	Negative	
Day 1	0.71	0.69	5.3 fM
Day 2	1.2	0.17	640 aM
Day 3	0.82	0.76	690 aM
Day 4	0.83	1.1	4.1 fM
Day 5	1.4	0.55	703 aM
Mean	0.99	0.66	

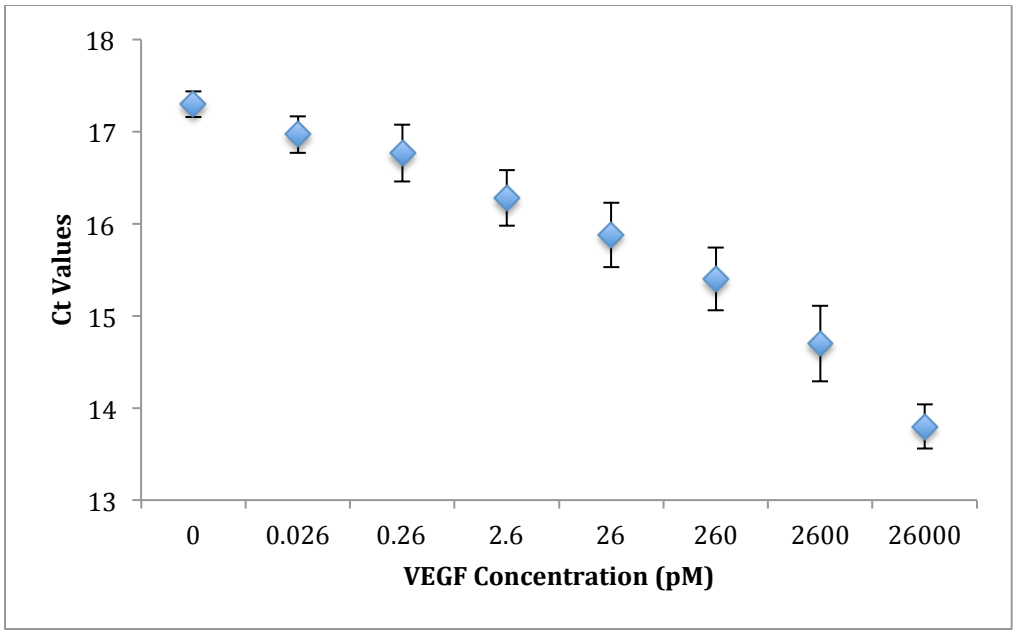

Figure 30: Data reproducibility. *Five experiments in PBS on five different days in 6 replicas (n=30) each were performed to confirm the reproducibility of data. The experiments were performed in PBS under conditions using the "One-step format". Error bars represent +/- 1 STDEV.*

2.9.22 Assay validation in complex clinical samples

For any clinically useful assay excellent analytical performance in clean buffer must be validated in more complex samples. VEGF was therefore spiked into serum and bronchoalveolar (BAL) fluid, two potential sample sources for diagnostic assays. Limits of detection were calculated to be 3.4 fM and 3.3 fM, respectively for the "avidin-phage" (**Figure 31**) and "antibody-phage" (**Figure 32**) approaches in diluted serum and 5.5 fM and 4.7 fM for the "avidin-phage" (**Figure 33**) and "antibody-phage" (**Figure 34**) approaches in diluted BAL fluid. These numbers are in good accordance with the numbers measured in PBS buffer, and suggest a low inherent non-specific binding of the modified phage reagent even in more complex backgrounds. In fact, we determined that out of

each million phage offered to the reaction, only 420 (+/- 160) bound non-specifically to antibody-functionalized magnetic capture particles ($5*10^6$) in PBS, 169 (+/- 7) in 20% serum, and 4707 (+/-314) in 50% BAL fluid. This corresponds to as low as 0.05-0.13 phage non-specifically bound per magnetic particle in PBS, 0.04-0.08 phage per particle in 20% serum, and 1-3 phage per particle in 50% BAL fluid.

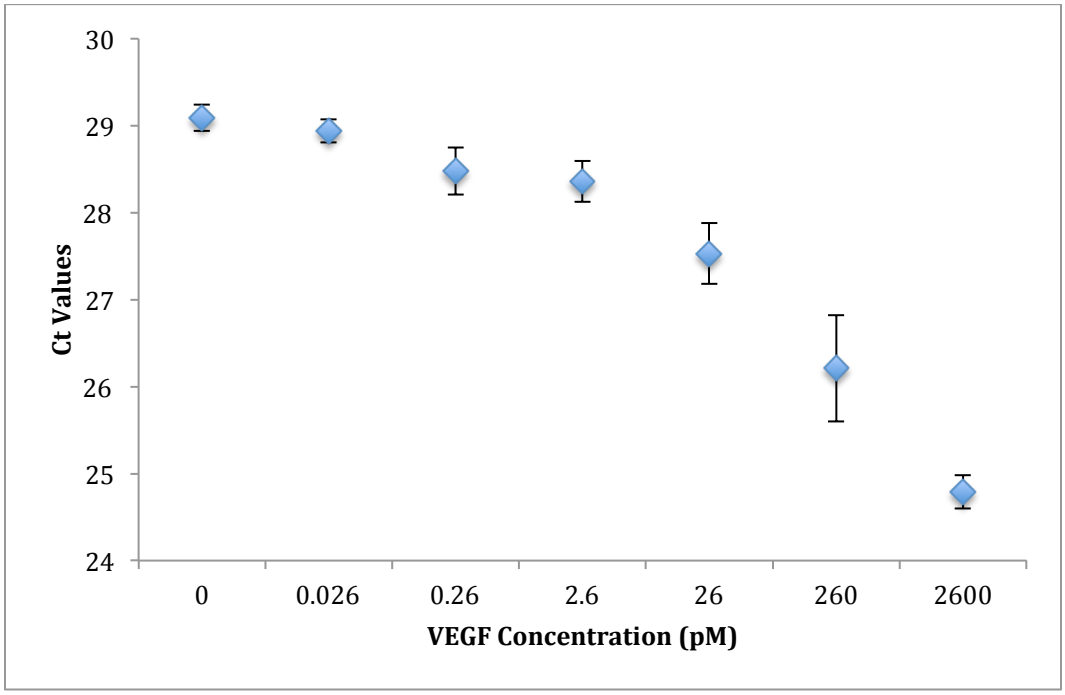

Figure 31: "Avidin-phage" assay in 20% serum. *VEGF detection in 20% serum using* **the** *pre-assembled avidin-phage construct; n=6, error bars = ±1 SD, NTC >35.*

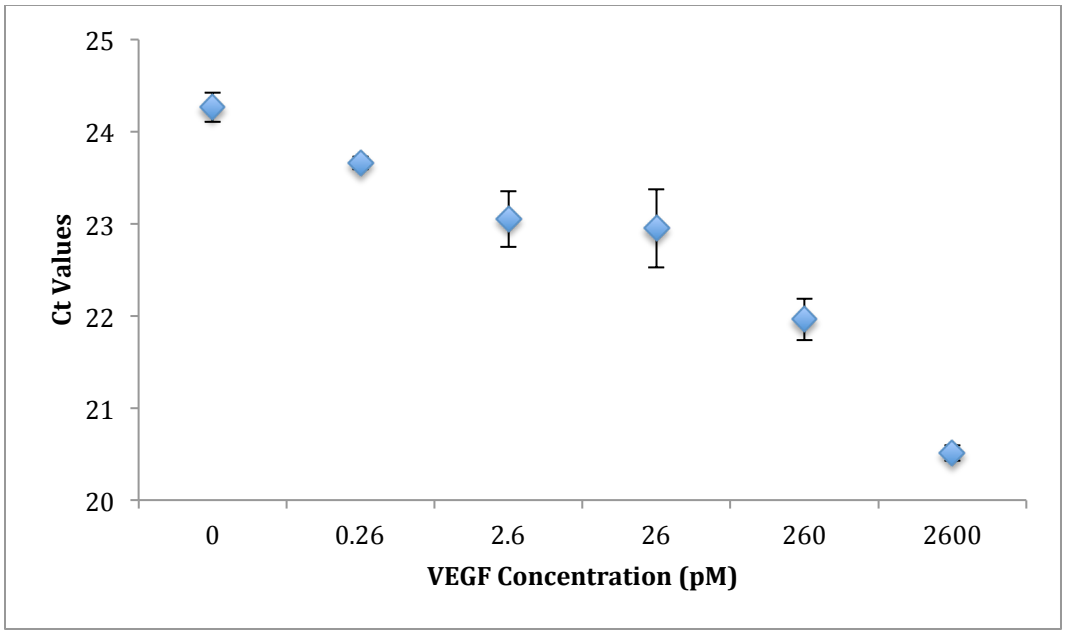

Figure 32: "Antibody-phage" assay in 20% serum. *VEGF detection in 20% serum using the antibody-phage format; n=6, error bars = ±1 SD, NTC >35.*

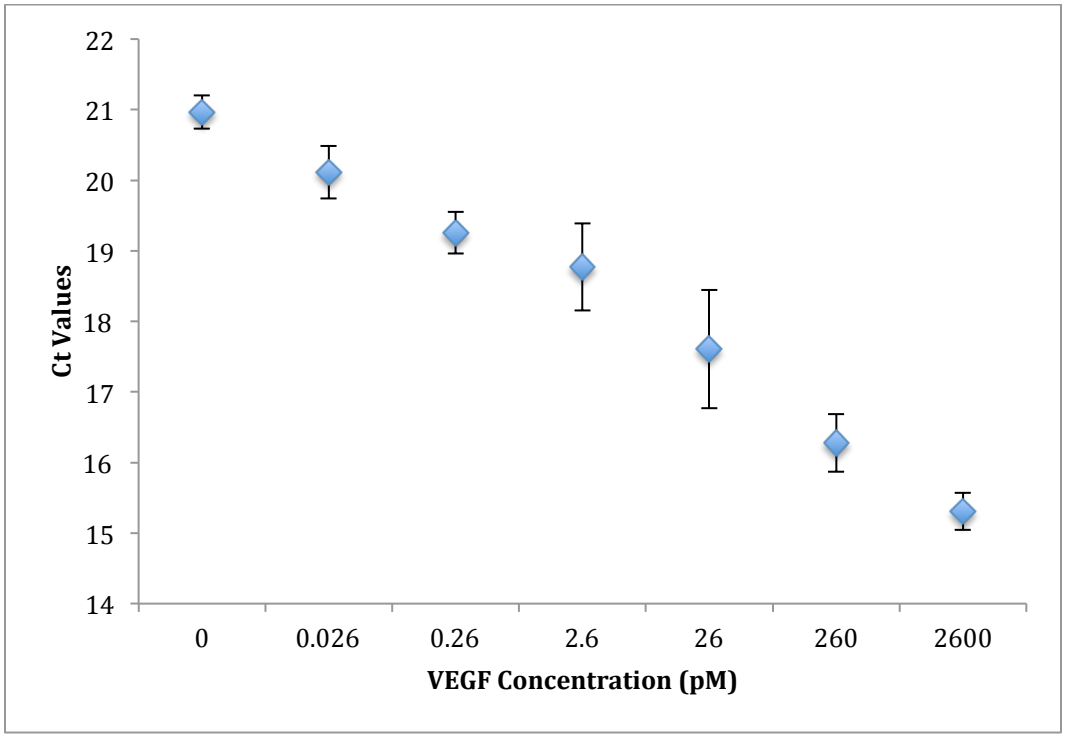

Figure 33: "Avidin-phage" assay in 50% BAL. *VEGF detection in 50% BAL using the pre-assembled avidin-phage construct; n=6, error bars = ±1 SD, NTC >35.*

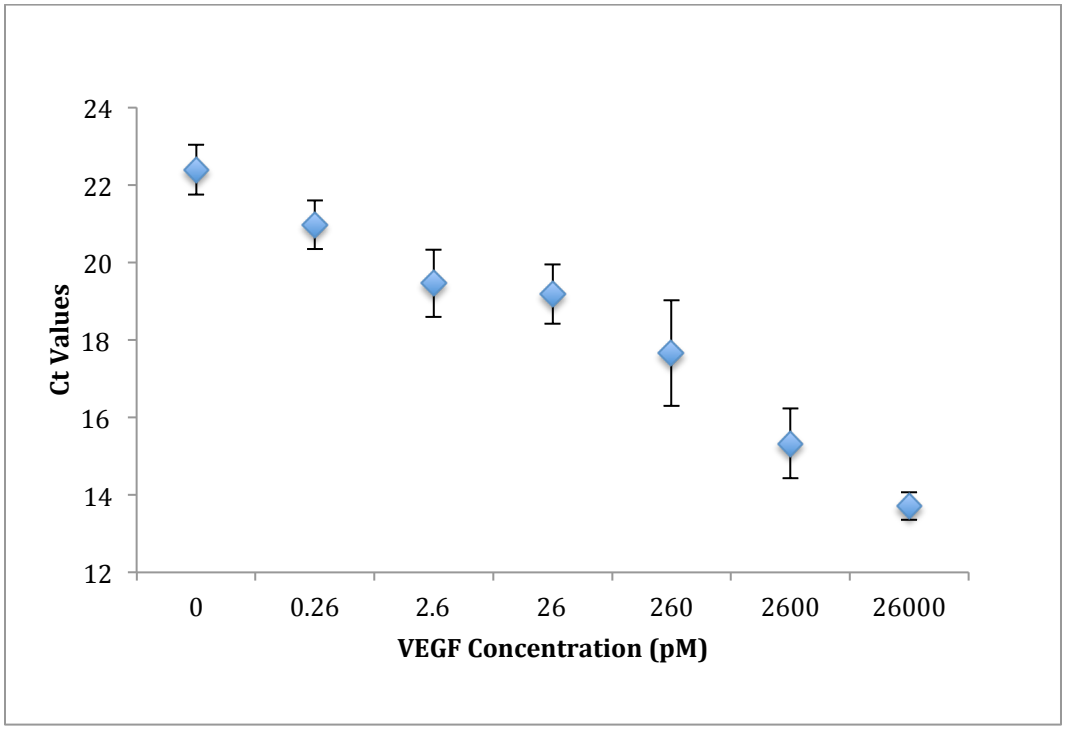

Figure 34: "Antibody-phage" assay in 50% BAL. *VEGF detection in 50% BAL using the antibody-phage format; n=6, error bars = ±1 SD, NTC >35.*

3 Chapter 3: Alumina Surface Modifications

A portion of this work has been described in Litvinov *et al.*, "Development of Pinhole-Free Amorphous Aluminum Oxide Protective Layers for Biomedical Device Applications," *Surface and Coating Technol*ogy, vol. 224, p. 101-108, 2013.

3.1 Introduction

Aluminum oxide or *alumina* films are well known for their high strength, corrosion resistance, insulating properties, and wear resistance. The material has been extensively characterized to support an ever-growing set of applications from mechanical to optical to electronic [69-73]. In this work, the application of ultra-thin pinhole-free layers of aluminum oxide for corrosion protection/electrical insulation of electromagnetic biosensor structures [74, 75] was explored. Conformal thin-film aluminum oxide layers were deposited using DC magnetron reactive sputtering to allow protection on non-planar geometries of biosensors to which biologically active molecules can be attached using surface-specific chemistry. The biosensors can be used for detection of biological agents in protein and DNA assays, in some cases mediated by the binding of phage reporters, as the basis of diagnostics in cancer or infectious diseases.

3.2 Alumina protective layer

3.2.1 Materials and methods for deposition of alumina

All materials synthesis and optical/e-beam lithography were done in a class 100 cleanroom to avoid wafer contamination. An ultra-high vacuum DC magnetron sputtering system (a base pressure of $1.33*10^{-7}$ Pa) was used for metal and aluminum oxide depositions. Two types of wafers, highly conductive p-doped silicon wafers (etched in 10% HF buffer solution to remove native oxide) and silicon wafers coated with a 500 nm-thick silicon oxide, were used as described below.

3.2.1.1 Aluminum oxide deposition

The AJA six-source UHV sputtering chamber equipped with AJA 2" sputtering guns in balanced magnet configuration was used. The depositions were done at room temperature. The 99.99% purity aluminum target was 3" in diameter. The center-to-center distance for metal deposition between the center of the sputtering target to the center of the wafer was 25 cm and the sputtering gun tilt was kept constant at 50 degrees off the wafer vertical direction. The sputtering system was calibrated for every target. Based on the time of deposition of a metal and the resulting thickness measured by Focused Ion Beam (FIB), the rate of deposition of aluminum was calculated to be equal to 5 nm/min.

Aluminum oxide deposition was preceded by sputter-deposition of a 1 nm aluminum layer in 0.67 Pa of Argon and post-deposition oxidized in O_2

plasma to form an aluminum oxide seed layer. Aluminum oxide was then deposited by reactive sputtering from a 99.99% purity aluminum target in an Ar/O_2 mixture in an ultra-high vacuum system. Oxygen plasma was generated from oxygen gas using a DC-powered ion source.

The deposition parameters were optimized to yield an aluminum oxide layer with the best protective/insulating properties: the deposition pressure (0.33 to 2.7 Pa at 35 sccm flow rate of Ar and varying O_2 partial pressure), oxygen partial pressure (flow rate between 3 and 7 sccm), sputtering gun power (50 to 200 W), substrate RF bias power (5W to 30 W), and deposition time (50 to 2000 sec) were varied to optimize the aluminum oxide properties.

Deposition conditions were varied to adjust film properties, which were characterized using Fourier Transform Infrared Spectroscopy (FTIR) and X-ray photoelectron spectroscopy (XPS). Spectroscopic ellipsometry was used to gauge the film thickness and the corresponding deposition rates. Corrosion protection/electrical insulation properties of the aluminum oxide films were evaluated using lithographically defined metallic device structures that were overcoated with the developed material, and then exposed to corrosive fluids.

It was found that the oxygen flow rate, which affects the partial pressure of oxygen in the processing gas, is the most critical parameter for a given deposition rate. Adjusting deposition rate (by increasing or decreasing the deposition power) required corresponding increase of decrease of the oxygen flow rate.

3.2.1.2 Oxygen Flow Rate Optimization

Aluminum oxide samples were prepared using DC magnetron sputtering at 10 W bias power and 100 W target power at various flow rates of oxygen. The samples show an increase in electroplating current with time for samples made with an oxygen flow rate of 5 sccm and lower. The samples made with an oxygen flow rate of 7 sccm show stable current, but are not reproducible due to spark generation from the aluminum target (due to target oxidation), resulting in film defects. The use of 6 sccm of oxygen produces reliable and reproducible results, with a low and stable electroplating current and no detectable deposition through pinholes. As a result, the pinhole-free aluminum oxide films were deposited at 10 W bias, 100 W aluminum deposition rate, 0.67 Pa process pressure, and 6 sccm flow rate of oxygen.

3.2.1.3 Corrosion resistance in PBS solutions

Two samples, one with a protective aluminum oxide layer (after UV/Ozone treatment) and another without any aluminum oxide layer, were placed in PBS solution for up to 72 h at 25°C with gentle shaking. The samples were removed from the solution and washed with deionized water to remove any trace of PBS. The state of the device structures at each stage was checked using SEM (FEI XL-30FEG scanning electron microscope equipped with NPGS (Nabity Pattern Generation Systems) for microscopic analysis and e-beam lithography pattern generation).

To further explore the protective properties of the aluminum oxide coatings, the samples exposed to PBS for different periods of time were tested

for presence of pin-holes. The samples were fully immersed in 100 mL of PBS solution for 24, 48, 72, and 96 h, then taken out, rinsed with deionized water, dried with nitrogen gas, and checked for pinholes using the electroplating assay. SEM images were taken to confirm the results. The copper plating was done using Picostat for current lower than 100 nA and Potentiostat for higher currents. The stimulator was set for "Pulse" mode with pulse sent every 1 millisecond for 30 seconds.

3.2.2 Results for alumina layer deposition

3.2.2.1 Deposition conditions

The use of flow rate of 6 sccm of oxygen was reliable and reproducible, with a low and stable electroplating current and no detectable deposition through pinholes. As a result, the pinhole-free aluminum oxide films were deposited at 10 W bias, 100 W aluminum deposition rate, 0.67 Pa process pressure, and 6 sccm flow rate of oxygen.

3.2.2.2 Corrosion resistance in PBS solutions

At zero time, before the sample was placed in PBS solution, the electroplating current was approximately equal to $2.5*10^{-7}$ A, a current that was generally noticed on the samples with tantalum and copper layers protected by aluminum oxide. The measured current of alumina-protected sample showed an increase of roughly two-fold per 24 h, reaching $1.5*10^{-6}$ A in 30 seconds for the sample of 72 h, but holding constant, indicating that no copper was depositing on the surface of the sample during electroplating. After 72 h in PBS solution, the current increased significantly during the first 30 seconds, indicating copper

plating on the area damaged by PBS. As can be seen in **Figure 35**, no visible damage was caused to the protected device structures after 72 h exposure to PBS.

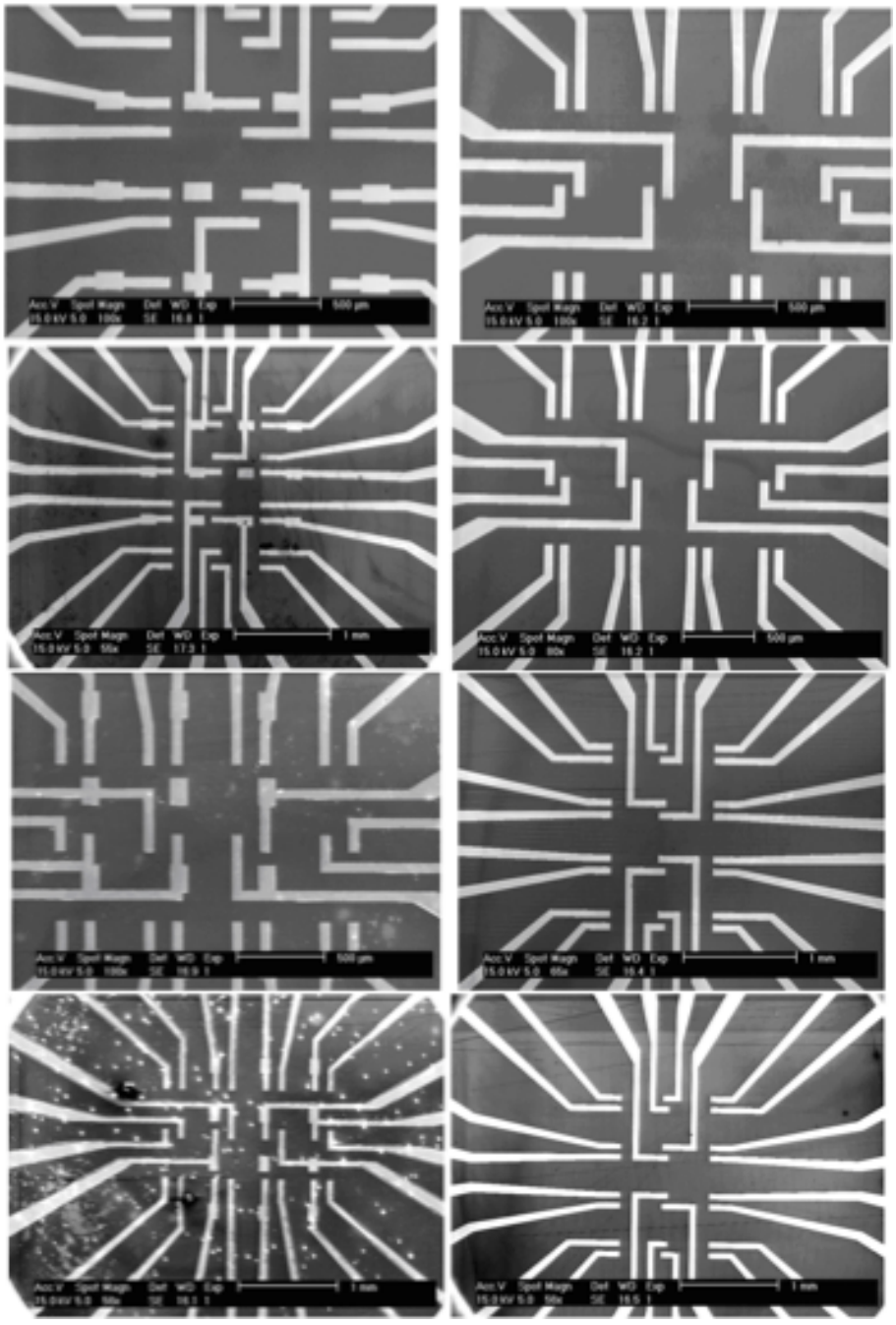

Figure 35: **Corrosion in PBS solution of device structures** *without (left) and with (right) protective aluminum oxide layer; from top to bottom: 4 h, 24 h, 48 h, 72 h.*

3.2.2.3 Protected Device Resistance Measurements

For the resistance measurements, a small current of 1 mA was applied to protected (Section 3.1) and unprotected samples. The results of the experiment are summarized in Table II. The resistance of the protected sample increased from 1.3 to 2.2 Ohms during the 72-hour period. This negligible increase in resistance indicates that the sample was protected for this period of time. During the last 24 h of the experiment shown (from 48 to 72 h), one can notice an increase in the protected sample's resistance from 1.5 to 2.2 Ohms. From this, it can be concluded that the life limit of the alumina film is approximately 48 h, which is sufficient for biofunctionalization and testing of the sensor. However, the data in Table 2 shows a higher corrosion level as well as broken sensors, indicating that the sample cannot withstand the applied current without proper protection layer.

Table 2: Resistance data of protected and unprotected samples.

Time (h)	Protected Sample Resistance (Ohms)	Unprotected Sample Resistance (Ohms)
0	1.3	1.3
4	1.3	4.8
24	1.4	161
48	1.5	162
72	2.2	infinite

A 25-nm thick amorphous pinhole-free corrosion-protective aluminum oxide layer was made using ultra-high vacuum DC magnetron sputtering. The best film quality was achieved at a flow rate of 6 sccm of oxygen and 35 sccm of argon, process pressure 0.67 Pa, bias power 20 W, and target sputtering power 20 W. It was found that unprotected sensors immersed in PBS showed a sharp increase in resistance due to corrosion, while protected sensors were relatively stable up to 72 h in saline PBS buffer. As a whole, the amorphous aluminum oxide film was proved to be an effective layer to protect the sensor from corrosion for at least 48 h after exposure to the biological solution, i.e., the PBS solution in this study. These results established that the alumina surfaces would be appropriate for surface functionalization for further experiments.

3.2.3 Materials and Methods for Alumina Surface Modification

Alumina surfaces were activated for protein immobilization with TESBA (triethoxsilylbutyraldehyde), which presents an aldehyde reactive with protein primary amines. The protocol for TESBA surface modification was always performed as following: Two percent TESBA in 95% ethanol (v/v) were mixed for 2 minutes. This step activated the TESBA compound for surface attachment, as shown in **Figure 36**. Silicon wafers with alumina coating were cut into small pieces (approximately 8*10 mm on a side) and immersed completely into 1 mL of prepared TESBA solution in 2 mL microcentrifuge tube. The samples were allowed to incubate on a shaker for 2 h at 25°C, and then washed with 95% ethanol, DI water, and PBS three times each to remove excess of silane compound.

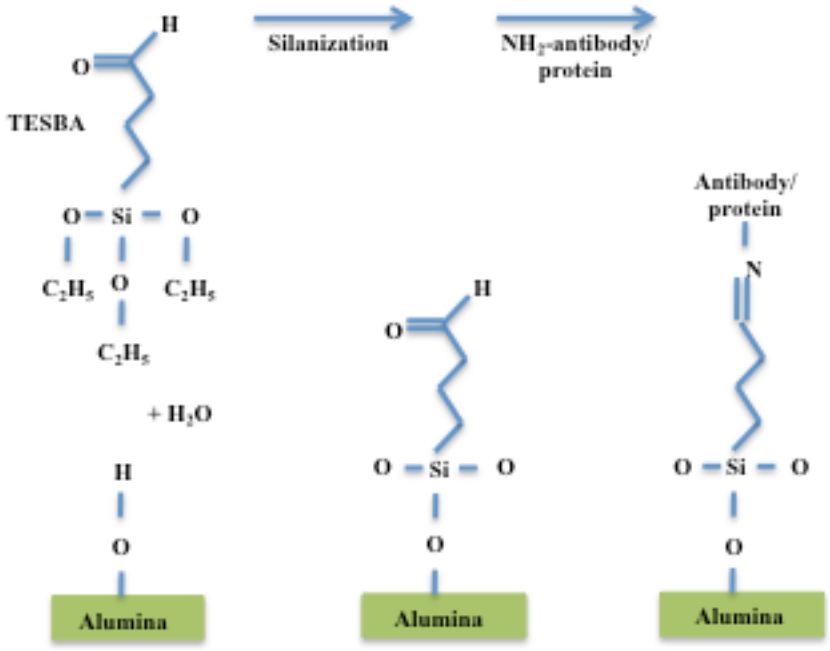

Figure 36: Aldehyde modification of alumina surfaces and antibody attachment. *Silanol groups are generated as a result of Triethoxysilylbutyraldehyde (TESBA) hydrolysis, and attachment to hydroxyl group on alumina surfaces. The disiloxane bond attaches butyraldehyde on alumina surface and carbonyl group of butyraldehyde reacts with the amino groups of the antibody to form a carbon–nitrogen double bond which immobilizes the antibody molecules through primary amines.*

3.2.3.1 Attachment of phage to anti-M13 antibodies on alumina surfaces

First, an experiment replicating the phage ELISA on Medisorb plate, as shown in **Figure 37**, was performed on TESBA-modified alumina surfaces (orange rectangle), where M13 AviTag phage (grey oval) were attached through mouse anti-M13 monoclonal antibodies (Y-shaped, violet) and detected using HRP-labeled goat anti-M13 monoclonal antibodies (Y-shaped, yellow, with green heptagon).

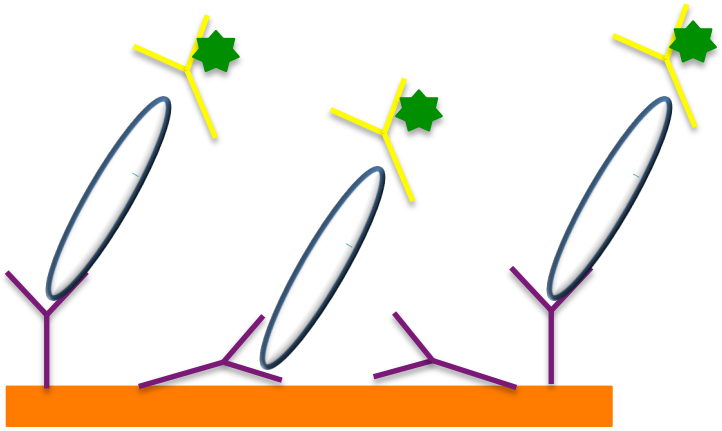

Figure 37: **Schematics of attachment of phage to alumina surface using TESBA chemistry.** *Phage (grey ovals) in serial dilutions was incubated on anti M13 monoclonal antibodies (purple, Y-shaped) attached to TESBA-modified alumina surfaces. The HRP-labeled anti-M13 monoclonal antibody was used for phage recognition. The detection was done with TMB ELISA and measured at 450 nm.*

The pre-cut alumina samples, 8x10 mm, in 2-mL microcentrifuge tubes were allowed to incubate on a shaker 2 h at 25°C, then washed with 95% ethanol, DI water, and PBS, three times each, to remove excess silane compound. Anti-M13 monoclonal antibodies (GE Healthcare, 27-9421-01), 1 µg/mL, 6.7 nM) were added in each tube and incubated in PBS on shaker for 2 h at 25°C. The samples were washes three times with PBS and blocked with 3% BSA in PBS 1 h at 37°C, after which they were washed in PBS 3 times. Phage dilutions from 10^{10} phage/mL to 10^{7} phage/mL (in 10 µL) were incubated on alumina surface for 2 h at 25°C on a gentle shaker and washed in PBS three times. HRP-labeled goat anti-M13 monoclonal antibodies (10 µL, 1:5000 dilution) were applied to the surface and incubated for 1 h at 25°C on an orbital shaker. The samples were washed and 10 µL TMB ELISA solution were applied

to the surface and allowed to develop for 20 minutes. The reaction was not stopped with H_2SO_4 as usual, but instead, measured in a NanoDrop instrument at 650 nm. No normalization at 405 nm was done to the OD values at 650 nm since the readout at 405 nm was near zero.

3.2.3.2 Attachment of "antibody-phage" constructs to VEGF on alumina surfaces

The next step after the attachment of phage molecules to alumina surfaces was to attach "antibody-phage" constructs through VEGF, as shown in **Figure 38**. The anti-VEGF polyclonal antibody (blue, Y-shaped) was immobilized on TESBA-activated alumina surfaces (orange rectangle) as described in Section 3.2.3. VEGF (yellow ovals) dilutions in PBS were made at concentrations from 2.6 nM to zero VEGF solutions and allowed to incubate for 2 h at 25°C and continue overnight at 4°C. The samples were washed with PBS three times and blocked with 3% BSA in PBS for 1 h at 37°C, after which they were again washed 3 times in PBS. Phage construct (10^{10} phage/mL, 10 μL volume, grey oval) were incubated on alumina surface for 2 h at 25°C on a gentle shaker and washed in PBS three times. Goat HRP-labeled anti-M13 monoclonal antibody (10 μL, 1:5000 dilution, blue Y-shape with green heptagon) was applied to the surface and incubated for 1 hour at room temperature on a gentle shaker. The samples were washed 3 times in PBS and 10 μL of TMB ELISA solution was applied to the surface and allowed to develop for 20 minutes. The reaction was not stopped with H_2SO_4 and was measured in the NanoDrop instrument at 650 nm. The same experiment was repeated with TESBA surface activation for 16 h at 25°C and overnight at 4°C.

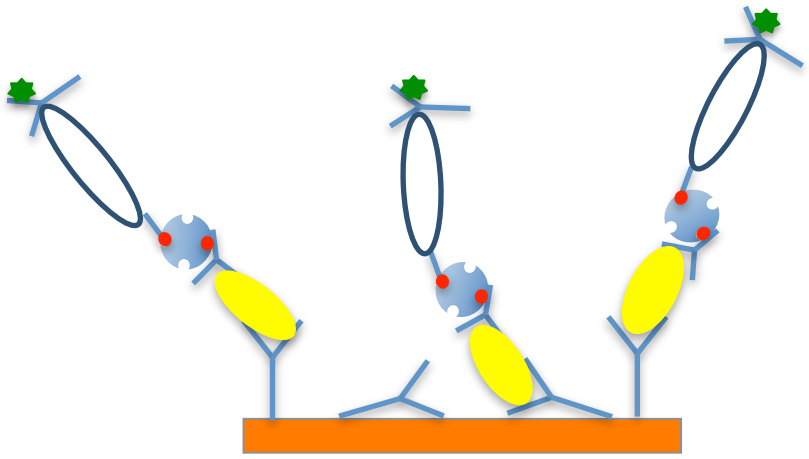

Figure 38: **Schematics of attachment of "antibody-phage" to TESBA-modified alumina surface through VEGF.** *Immuno-phage construct was capruted from solution by VEGF (yellow ovals) attached to anti-VEGF polyclonal antibody (blue, Y-shaped) immobilized on alumina surfaces (orange rectangle). The phage construct was recognized by HRP-labeled anti M13 monoclonal conjugate and detected using TMB ELISA at 450 nm.*

3.2.3.3 Protein A/G-oriented antibody immobilization

Protein A/G is known to properly orient antibodies on modified surfaces [76, 77]. Since antibodies attach to surfaces through a number of amino acids, it may lead to partial or full loss of antibody activity and unavailability of active sites. A fusion of protein A and protein G should be used for antibody immobilization because it has the highest affinity to the heavy chain of the Fc region of an antibody [78]. The experiment utilizes two different antibodies. The first, mouse polyclonal anti-VEGF antibody, has to have a strong binding with protein A/G, while the second, HRP-labeled, should have low or no binding at all to protein A/G to prevent cross-linking. The secondary antibodies that were available to use with this assay had strong binding to protein A/G and it was decided to substitute the HRP-labeled antibody with HRP-labeled Streptavidin.

100 μL 1 mg/mL protein A/G and 100 μL PBS were adsorbed on MediSorb ELISA plates for 2 h at 25°C on a shaker and washed 3 times with PBS. Anti-VEGF polyclonal antibody was immobilized in wells at 1μg/ml for 2 h at 25°C on a shaker and washed 3 times in PBS. VEGF in concentrations from 2.6 nM to 26 fM, and zero, in PBS was incubated on the plate for 2 h on shaker at room temperature, then washed 3 times with PBS and blocked with 3% BSA for 2 h at room temperature on a shaker. After three washes with PBS, biotinylated Lucentis (5 μg/mL) was incubated for 2 h at room temperature and washed 3 times with PBS. 100 μL HRP-labeled Streptavidin was added at a 1:500 dilution (manufacturer's protocol) for 1 hour and washed 3 times with PBS. 100 μL of TMB ELISA solution was added to the wells and allowed to develop for 35-40 min. 50 μL of 2 M H_2SO_4 were added to stop the reaction and the signal was measured in the NanoDrop instrument at 450 nm.

Figure 39 shows the schematics of this assay. On TESBA-functionalized surfaces (orange), protein A/G (blue) was immobilized, followed by the attachment of polyclonal anti-VEGF antibodies (blue), VEGF (yellow) and biotinylated Lucentis (blue with red dot). The detection was done using HRP-labeled Streptavidin (blue circle with green heptagon).

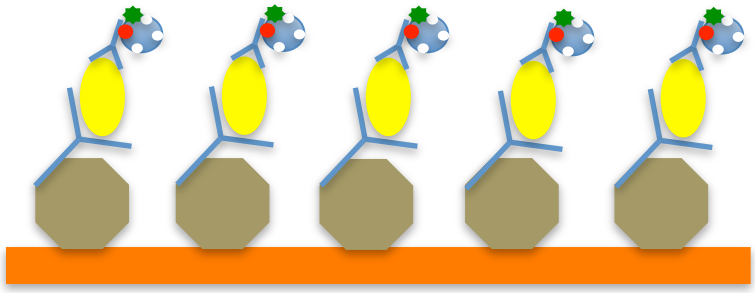

Figure 39: **Schematic representation of polyclonal anti-VEGF antibody attachment to TESBA-modified surfaces in the presence of protein A/G.** *Protein A/G (brown octagons) was immobilized on TESBA-modified alumina surfaces (orange rectangle), followed by polyclonal anti-VEGF antibodies (blue, large Y-shapes), VEGF (yellow ovals) in dilutions, and biotinylated Lucentis (blue, small Y-shapes with red dot representing biotin); HRP-labeled streptavidin was used to recognize the biotinylated antibody and the detection was done with TMB-ELISA.*

3.2.3.4 Attachment of protein A/G to TESBA-activated alumina surfaces

The next experiment was performed on alumina surfaces to compare the results of ELISA to modified alumina. Alumina surfaces were activated with TESBA and immersed in 1 mL of 1 μg/mL of protein A/G or PBS and incubated on a shaker for 2 h at 25°C, then washed 3 times with PBS. The attachment of anti-VEGF antibody, VEGF, biotinylated Lucentis, and HRP-labeled Streptavidin were as describes in Section 3.2.3.3. The samples were immersed in 500 μL TMB and allowed to develop for 20 minutes. The samples were then taken out of the solution and 250 μL of 2 M H_2SO_4 were added to stop the reaction. The volumes of liquid were scaled up from the original ELISA procedure to match the previous experiment on the ELISA plate.

3.2.4 Results for attachment of biomolecules to alumina surfaces

3.2.4.1 Capture of phage on alumina surface

In this experiment, M13 AviTag phage were attached to TESBA-modified alumina surfaces through a monoclonal anti-M13 antibody and a HRP-labeled anti-M13 monoclonal conjugate was used as a label for a colorimetric ELISA, as shown in **Figure 40**. The background for zero-phage sample was equal to 0.14 and the signal for 10^{10} phage/mL was 0.93.

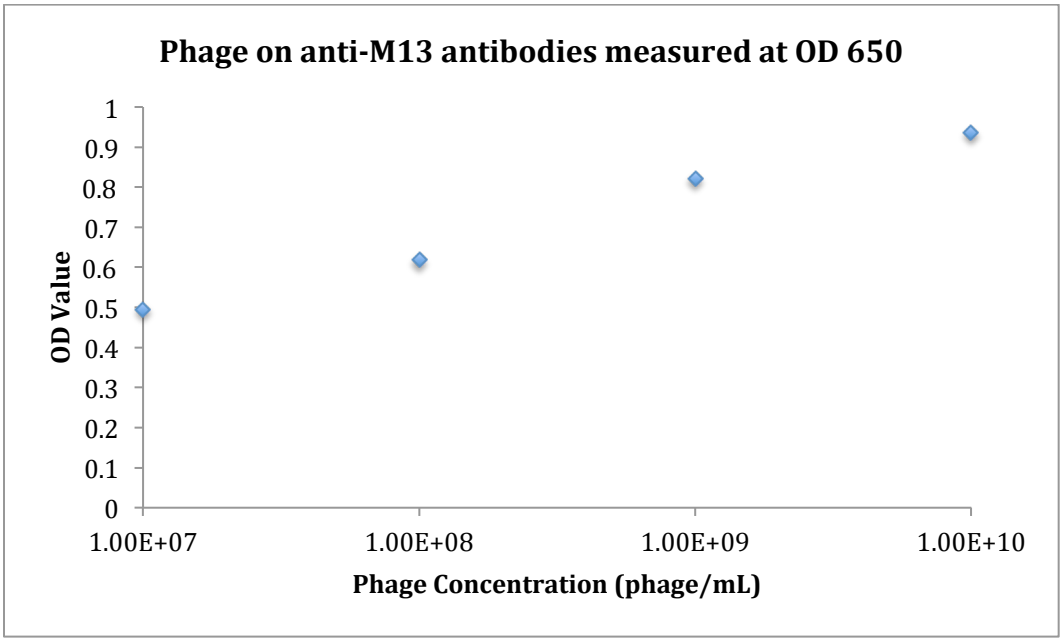

Figure 40: ELISA for M13 phage detection on alumina surface *(n=1). Phage in serial dilutions was incubated on anti-M13 monoclonal antibody immobilized on alumina sirfaces. The detection was done with HRP-labeled anti-M13 monoclonal antibody. No-phage sample at OD 650 was equal to 0.14.*

3.2.4.2 Attachment of phage construct to alumina

In this experiment, biotinylated phage construct in the "antibody-phage" format was attached to the TESBA-modified alumina surfaces. Two experiments

with different times of TESBA surface functionalization (2 h and overnight) were performed. As seen in **Figure 41**, for 2 h of TESBA activation, the OD value at 650 nm wavelength for the highest VEGF concentration was below 0.3. The background measured at zero VEGF concentration was equal to 0.1. The limit of detection of the phage construct was approximated using logarithmic fit and was equal to 420 fM. On the other hand, the overnight TESBA activation of alumina surfaces shows that the signal from the highest VEGF concentration was equal to 0.52. The background signal at zero VEGF concentration was equal to 0.1. As estimated from Figure 40, the limit of detection for this experiment was 204 fM. The signal improvement was not significant (if any at all) when comparing the two experiments with the OD signal of M13 phage on the alumina surface coupled through a monoclonal anti-M13 antibody. The reason for this might be differences in surface coverage between anti-VEGF and anti-M13 antibodies, different need for incubation times, or, optimization of TESBA surface modification time.

3.2.4.3 Oriented antibody immobilization with protein A/G on ELISA plate

After the experiments with time of TESBA surface modification, it seemed that the time of TESBA activation did not change the signal significantly; it was still very low, with the highest signal being just above 0.5. The next step in determining why the OD signal in the experiment shown in Figure 40 was so low was to check the efficiency of attachment of polyclonal anti-VEGF antibody to the alumina surfaces. An experiment for protein A/G attachment to ELISA plates prior to incubation of polyclonal anti-VEGF

antibody was performed. Protein A/G was adsorbed on ELISA plates, followed by three PBS washes ant incubation of polyclonal anti-VEGF antibody.

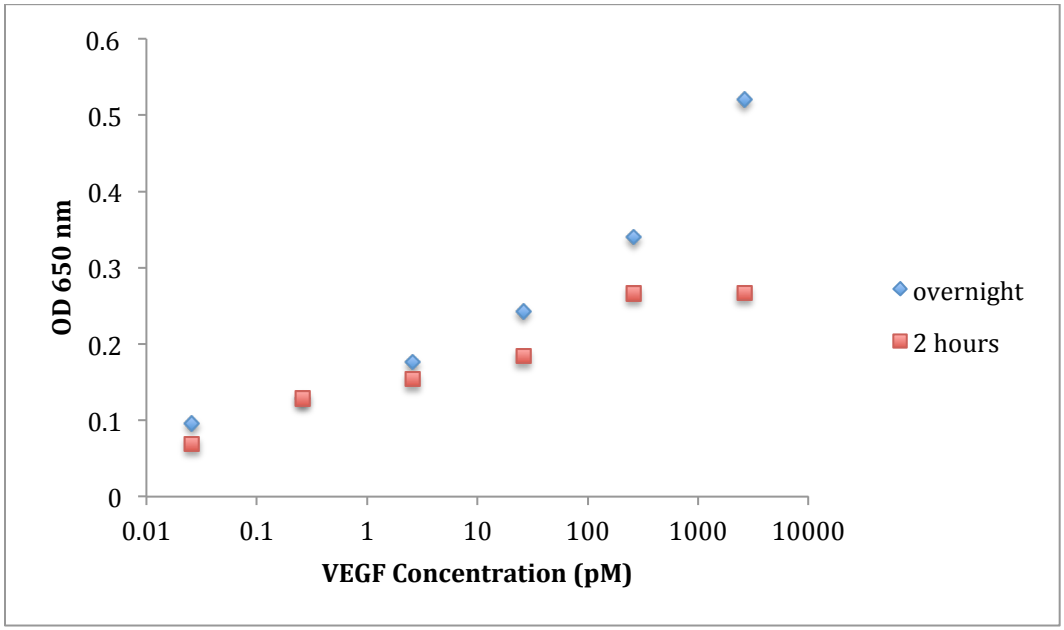

Figure 41: **Comparison of two hours and overnight incubation of TESBA on alumina surfaces.** *Alumina surface was activated with TESBA for different times, after which polyclonal anti-VEGF antibody, VEGF, and immuno-phage construct were incubated in layers with washes between each layer. The signal was detected using colorimetric ELISA at OD 650.*

In the case when protein A/G was omitted from the protocol, polyclonal anti-VEGF antibody was adsorbed on the ELISA plate. VEGF at various concentrations was incubated, followed by 3 PBS washes and blocking with 3% BSA. After washing, biotinylated Lucentis was added to the plate, followed by wash and incubation of HRP-labeled Streptavidin. The read-out of the assay was colorimetric ELISA at 450 nm wavelength.

We observed no major difference between protein A/G adsorption followed by immobilization of polyclonal anti-VEGF antibody and polyclonal anti-VEGF antibody adsorption directly on the plate without protein A/G. As

shown in **Figure 42**, the signal for zero VEGF, though, was close to 0.1 in both cases, which is approximately only twice as high as a regular background signal (0.05), produced by 100 uL of TMB ELISA and 50 uL of H_2SO_4.

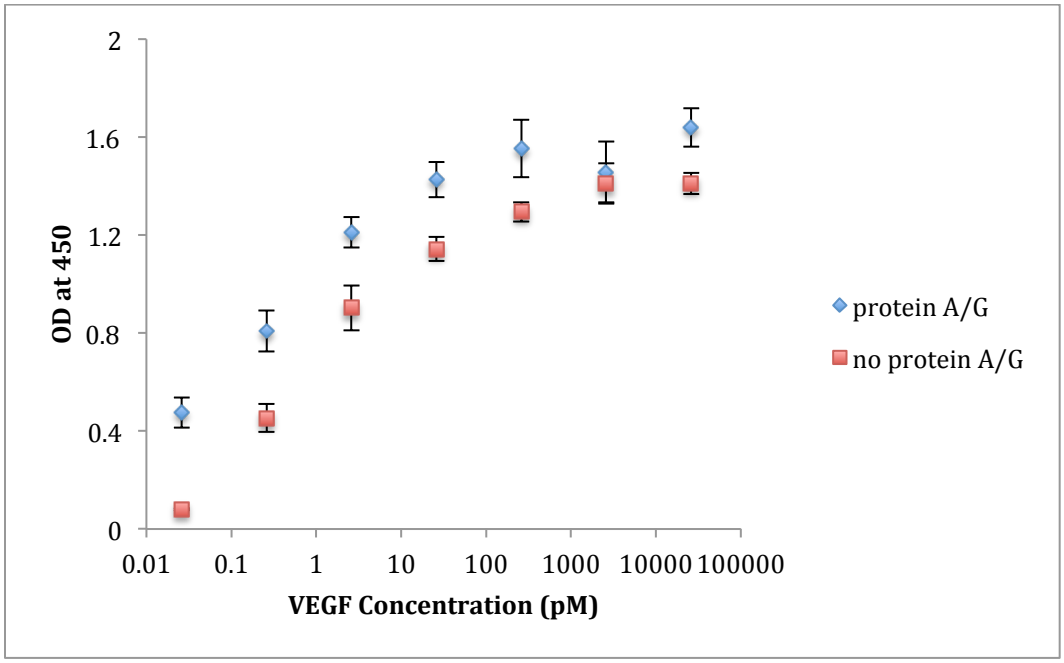

Figure 42: Immobilization of anti-VEGF antibody on ELISA plate with and without immobilization of protein A/G *(n=2). Protein A/G was immobilized in microplate wells, after which polyclonal anti-VEGF antibody, VEGF in serial dilutions, Lucentis, and HRP-labeled Streptavidin were added in layers with washes between them. The signal was detected with colorimetric ELISA at OD 450 nm.*

3.2.4.4 Oriented antibody immobilization with protein A/G on alumina surfaces

Exactly the same experiment as described in Section 3.2.4.5 was performed on TESBA-modified alumina surfaces. Protein A/G was immobilized on TESBA-activated alumina surfaces, after which polyclonal anti-VEGF antibody, VEGF in serial dilutions, Lucentis, and HRP-labeled Streptavidin were added in layers with washes between them. After immobilization of protein A/G,

the anti-VEGF antibody was properly oriented, which allowed a better target recognition, probably, due to availability of more antibodies' binding sites. The specific binding of VEGF was higher, due to proper antibody orientation, which resulted in OD signal increase for higher VEGF concentrations. Those concentrations (also in PCR assays), were always problematic due to not enough antibody attachments to the surface of alumina (and magnetic particles in PCR). Since more properly oriented antibodies are available, more of VEGF molecules can be attached to them, thus, with this assay, a higher signal can be detected. As can be seen on **Figure 43**, there was a major difference in signal corresponding to the highest VEGF concentration with protein A/G immobilization (OD_{450} = 2.15 for 26 nM and for zero VEGF was 0.21), while for "no protein A/G," the signal ranged only from 0.53 to 0.24 for no-VEGF control. The background in both cases was higher that the one on ELISA plate, probably, due to difference in surfaces. The detection limit of this assay was 7.2 pM.

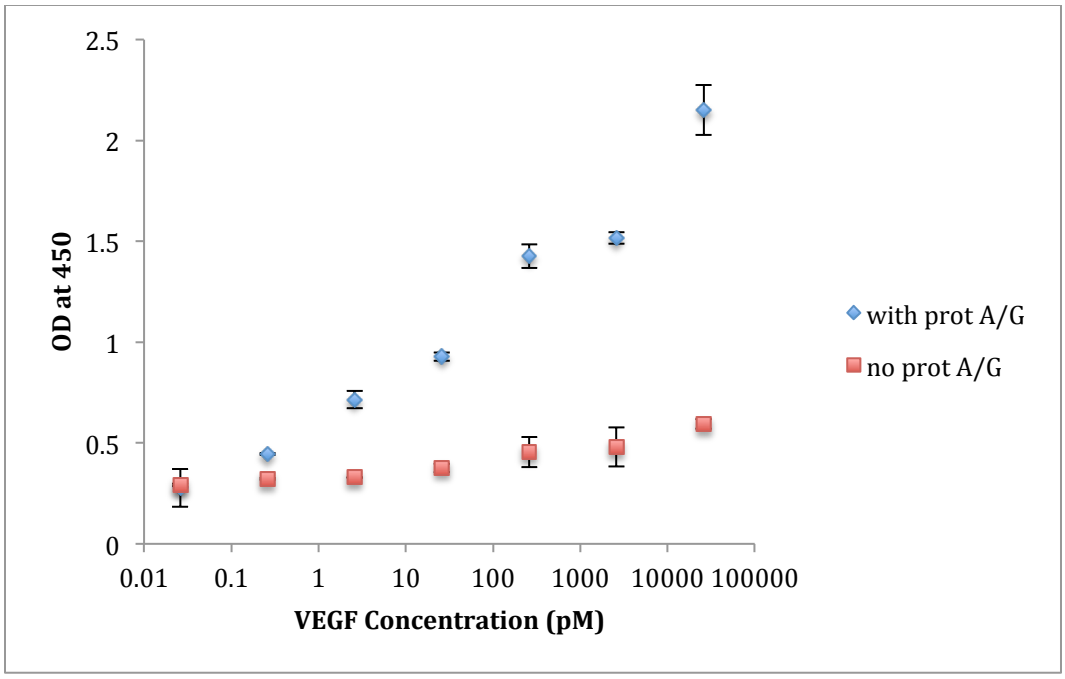

Figure 43: Immobilization of anti-VEGF antibody on alumina surfaces with and without immobilization of protein A/G *(n=2). Protein A/G was immobilized on TESBA-activated alumina surfaces, after which polyclonal anti-VEGF antibody, VEGF in serial dilutions, Lucentis, and HRP-labeled Streptavidin were added in layers with washes between them. The signal was detected with colorimetric ELISA at OD 450 nm.*

4 Conclusions and Suggestions for Future Work

4.1 Summary

In the work described in Chapter 2, VEGF was concentrated from spiked samples (PBS, 20% serum, and 50% bronchoalveolar lavage fluid, BAL) using antibody functionalized magnetic particles, and detected by phage functionalized with a second antibody. The read-out of the assay is conducted by quantitative real-time PCR amplification of the reporter phage DNA. Various experimental approaches were used to achieve the highest sensitivity and specificity through optimization of sample preparation, wash procedures, and assay technique. In all experiments, VEGF could be reproducibly detected at femtomolar levels in PBS, 50% BAL, and 20% serum.

In Chapter 3, the attachment of antibody-phage construct and VEGF molecules in PBS to alumina surfaces as the basis of phage-mediated biosensing was achieved using TESBA surface chemistry. The read-out of this assay was a colorimetric ELISA with HRP-labeled monoclonal anti-M13 antibodies or HRP-labeled Streptavidin. Using protein A/G to properly orient the anti-VEGF antibody on the TESBA surface resulted in a limit of detection of 7.2 pM in PBS.

4.2 Suggestions for future work

We developed an extremely sensitive assay, using convenient avidin-mediated assembly of PCR reporter reagents. In real-time PCR, we were only able to obtain a difference of 6 Ct values between the highest VEGF concentration and the no-VEGF control. The VEGF concentrations ranged from

nano- to attomolar, corresponding to approximately 10^{12} to 10^{5} molecules per reaction. When providing 10^{9} phage particles per sample, assuming one-to-one binding of phage to VEGF, one would expect a better correlation of phage-per-VEGF to Ct values. For example, for a difference of seven orders of magnitude in VEGF concentration, one would expect at least 6 orders of magnitude difference in the phage PCR signal, which would correspond to up to 18 Ct values, and not six. Such an assay is not good at discriminating fine differences among concentrations, though it is excellent for detecting yes/no targets such as pathogens or cancer-generated unnatural fusion proteins at very low levels. However, based on other published works, the 4-8 values in delta Ct are what other groups see, performing similar detection approaches and using similar reagents.

This leads to the hypothesis that one (or more) of the reagents did not have the proper binding to others, resulting only in thousandth of a percent binding, leaving us to investigate the reasons for the unexpected assay performance. First, the entire assay showed a much better behavior when performed on an ELISA plate, suggesting that the particles with their surface modification were the problem. However, only three different magnetic particles types (Sera particles, Tosyl MyOne, and carboxyl) with different surface chemistries were investigated during the experiments. While the non-specific binding of the no-VEGF control was improved, the binding of the higher VEGF concentrations did not increase.

Another issue we investigated is the stability of reagents. It was determined that the all reagents are best kept in their most concentrated form at 4°C. Moreover, we stored the AviTag phage with azide and antibiotics to prevent bacterial growth. While concentrated biotinylated phage showed a reasonable stability for at least 2 months, the phage construct was only stable for 5 days. The VEGF recognition antibody (Lucentis) is stable after biotinylation for at least 2 months. The biotinylated antibody/NeutrAvidin/biotinylated phage complex should be made fresh every week. The magnetic particles were stable. The particle surface functionalization was performed at least every other month, but there was no difference in experiment's performance when freshly functionalized particles were compared with the 2-months old particles.

In an effort to improve the assay, more experiments can be done with different types of magnetic particles and different surface chemistries. Three types of magnetic particles (SeraBeads, Tosyl MyOne, and NanoMag) with different surface chemistries for antibody attachment were investigated so far. It was found in Chapter 3, that protein A/G on TESBA-modified alumina surfaces improved the orientation of antibodies on surface, thus, leading to a higher detection signal. This technique may be added to the protocol for magnetic particles surface modification in an effort to orient the antibodies properly and have higher amounts of VEGF binding to the particles.

Another valuable extension would be to multiplexing, i.e. the detection of more than one target molecule with immuno-phage particle built with appropriate target-recognition antibodies. In this case, DNA of the phage would

be used as a template for quantitative real-time PCR. Multiplex detection of proteins can be achieved using immuno-phage particles decorated with different antibodies and containing unique DNA reporter sequences that can be detected in parallel using TaqMan® probes with different fluorophores.

References

[1] A. Jemal, R. Siegel, J. Xu, E. Ward, "Cancer statistics, 2010," *CA: A Cancer Journal for Clinicians,* vol. 60, pp. 277-300, 2010.

[2] M. Polanski, N. L. Anderson, "A list of candidate cancer biomarkers for targeted proteomics," *Biomarker Insights,* vol. 1, pp. 1-48, 2007.

[3] K. R. Kozak, F. Su, J. P. Whitelegge, K. Faull, S. Reddy, R. Farias-Eisner, "Characterization of serum biomarkers for detection of early stage ovarian cancer," *Proteomics,* vol. 5, pp. 4589-4596, 2005.

[4] B. Laxman, D. S. Morris, J. Yu, J. Siddiqui, J. Cao, R. Mehra, "A first-generation multiplex biomarker analysis of urine for the early detection of prostate cancer," *Cancer Research,* vol. 68, pp. 645-649, 2008.

[5] A. Vlahou, C. Laronga, L. Wilson, B. Gregory, K. Fournier, D. McGaughey, "A novel approach toward development of a rapid blood test for breast cancer," *Clinical Breast Cancer,* vol. 4, pp. 203-209, 2003.

[6] C. Birse, S. Ruben, L. Marcia, M. Mehdi, "Lung cancer markers and uses thereof," USA Patent, US Patent No: 7,892,760, 2007.

[7] T. M. H. Niers, "Coagulation, angiogenesis, and cancer," in *Dissertation*, ed. Digital Academic Depository, 2008.

[8] S. X. Leng, J. E. McElhaney, J. D. Walston, D. Xie, N. S. Fedarko, G. A. Kuchel, "ELISA and multiplex technologies for cytokine measurement in inflammation and aging research," *Journals of Gerontology Series A: Biological Sciences and Medical Sciences,* vol. 63, pp. 879-884, 2008.

[9] T. Sano, C. L. Smith, C. R. Cantor, "Immuno-PCR: very sensitive antigen detection by means of specific antibody-DNA conjugates," *Science,* vol. 258, pp. 120-122, 1992.

[10] N. Malou, D. Raoult, "Immuno-PCR: a promising ultrasensitive diagnostic method to detect antigens and antibodies," *Trends Microbiology,* vol. 19, pp. 295-302, 2011.

[11] M. Adler, R. Wacker, C. M. Niemeyer, "Sensitivity by combination: immuno-PCR and related technologies," *Analyst,* vol. 133, pp. 702-718, 2008.

[12] I. Burbulis, K. Yamaguchi, R. Yu, O. Resnekov, R. Brent, "Quantifying small numbers of antibodies with a 'near-universal' protein-DNA chimera," *Nature Methods,* vol. 4, pp. 1011-1013, 2007.

[13] J. Barletta, A. Bartolome, N. T. Constantine, "Immunomagnetic quantitative immuno-PCR for detection of less than one HIV-1 virion," *Journal of Virological Methods,* vol. 157, pp. 122-32, 2009.

[14] J. M. Nam, C. S. Thaxton, C. A. Mirkin, "Nanoparticle-based bio-bar codes for the ultrasensitive detection of proteins," *Science,* vol. 301, pp. 1884-1886, 2003.

[15] C. S. Thaxton, R. Elghanian, A. D. Thomas, S. I. Stoeva, J. S. Lee, N. D. Smith, "Nanoparticle-based bio-barcode assay redefines "undetectable" PSA and biochemical recurrence after radical prostatectomy," *Proceedings of the Natural Academy of Sciences of the U. S. A.,* vol. 106, pp. 18437-42, 2009.

[16] C. M. Lee, N. Iorno, F. Sierro, D. Christ, "Selection of human antibody fragments by phage display," *Nature Protocols,* vol. 2, pp. 3001-3008, 2007.

[17] G. P. Smith, "Filamentous fusion phage: novel expression vectors that display cloned antigens on the virion surface," *Science,* vol. 228, pp. 1315-7, 1985.

[18] Y. C. Guo, Y. F. Zhou, X. E. Zhang, Z. P. Zhang, Y. M. Qiao, L. J. Bi, "Phage display mediated immuno-PCR," *Nucleic Acids Research,* vol. 34, p. e62, 2006.

[19] H. J. Kim, M. A. Rossotti, K. C. Ahn, G. G. Gonzalez-Sapienza, S. J. Gee, R. Musker, "Development of a noncompetitive phage anti-immunocomplex assay for brominated diphenyl ether 47," *Analytical Biochemistry,* vol. 401, pp. 38-46, 2010.

[20] H. J. Kim, K. C. Ahn, A. Gonzalez-Techera, G. G. Gonzalez-Sapienza, S. J. Gee, B. D. Hammock, "Magnetic bead-based phage anti-immunocomplex assay (PHAIA) for the detection of the urinary biomarker 3-phenoxybenzoic acid to assess human exposure to pyrethroid insecticides," *Analytical Biochemistry,* vol. 386, pp. 45-52, 2009.

[21] H. J. Kim, M. McCoy, S. J. Gee, G. G. Gonzalez-Sapienza, B. D. Hammock, "Noncompetitive phage anti-immunocomplex real-time polymerase chain reaction for sensitive detection of small molecules," *Analytical Chemistry,* vol. 83, pp. 246-53, 2011.

[22] M. D. Scholle, J. W. Kehoe, B. K. Kay, "Efficient construction of a large collection of phage-displayed combinatorial peptide libraries," *Combinatorial Chemistry and High Throughput Screening,* vol. 8, pp. 545-51, 2005.

[23] M. D. Scholle, U. Kriplani, A. Pabon, K. Sishtla, M. J. Glucksman, B. K. Kay, "Mapping protease substrates by using a biotinylated phage substrate library," *Chembiochem,* vol. 7, pp. 834-838, 2006.

[24] M. D. Scholle, F. R. Collart, B. K. Kay, "In vivo biotinylated proteins as targets for phage-display selection experiments," *Protein Expression and Purification,* vol. 37, pp. 243-252, 2004.

[25] S. C. Suarez, M. Pieren, L. Cariolato, S. Arn, U. Hoffmann, A. Bogucki, C. Manlius, J. Wood, K. Ballmer-Hofer, "A VEGF-A splice variant defective for heparan sulfate and neuropilin-1 binding shows attenuated signaling through VEGFR-2," *Cellular and Molecular Life Sciences,* vol. 63, pp. 2067-2077, 2006.

[26] S. Takano, Y. Yoshii, S. Kondo, H. Suzuki, T. Maruno, S. Shirai, T. Nose, "Concentration of Vascular Endothelial Growth Factor in the Serum and Tumor Tissue of Brain Tumor Patients," *American Association for Cancer Research,* vol. 56, pp. 2185-2190, 1996.

[27] Z. J. Shang, J. R. Li, Z. B. Li, "Circulating levels of vascular endothelial growth factor in patients with oral squamous cell carcinoma," *International Journal of Oral & Maxillofacian Surgery,* vol. 31, pp. 495-498, 2002.

[28] R. Kolly, M. A. Thiel, T. Herrmann, A. Pluckthun, "Monovalent antibody scFv fragments selected to modulate T-cell activation by inhibition of CD86-CD28 interaction," *Protein Engineering,* vol. 20, pp. 91-98, 2007.

[29] F. A. Predonzani, F. Arnoldi, A. López-Requena, O. R. Burrone, "In vivo site-specific biotinylation of proteins within the secretory pathway using a single vector system," *BMC Biotechnology,* vol. 8:41, 2008.

[30] N. Ferrara, T. Davis-Smyth, "The Biology of Vascular Endothelial Growth Factor," *Endocrine Reviews,* vol. 18, pp. 4-25, 1997.

[31] C. Wiesmann, H. W. Christinger, A. G. Cochran, B. C. Cunningham, I. J. Wayne, J. Fairbrother, C. J. Keenan, G. Meng, A. M. de Vos, "Crystal structure of the complex between VEGF and a receptor-blocking peptide," *Biochemistry,* vol. 37, pp. 17765-17772, 1998.

[32] M. D. Miller, M. J. Benedik, M. C. Sullivan, N. S. Shipley, K. L. Krause, "Crystallization and preliminary crystallographic analysis of a novel nuclease from Serratia marcescens," *Journal of Molecular Biology,* vol. 222, pp. 27-30, 1991.

[33] J. E. Park, N. Ferrara, "The Vasculat Endothelial Growth Factor (VEGF) isoforms: Differential Deposition into the Subepithelial Extracellular

Matrix and Bioactivity of Extracellular Matrix-bound VEGF," *Molecular Biology of the Cell,* vol. 4, pp. 1317-1326, 1993.

[34] S. C. Suarez, M. Pieren, L. Cariolato, S. Arn, U. Hoffmann, A. Bogucki, "A VEGF-A splice variant defective for heparan sulfate and neuropilin-1 binding shows attenuated signaling through VEGFR-2," *Cellular and Molecular Life Sciences,* vol. 63, pp. 2067-2077, 2006.

[35] N. Ferrara, L. Shams, N. Lowman, H. K. Robert, "Development of Ranibizumab, An Anti-Vascular Endothelial Growth Factor Antigen Binding Fragment, As Therapy for Neovascular Age-Related Macular Degeneration," *Retina,* vol. 8, pp. 859-870, 2006.

[36] M. La Cour, "Intravitreal VEGF-inhibitors: is Avastin®a generic substitute for Lucentis®?," *Acta Ophthalmologica Scandinavica,* vol. 85, pp. 2-4, 2007.

[37] H. B. Lowman, "Therapeutic Anti-VEGF Antibodies," *Experimental Pharmacology,* vol. 181, pp. 131-150, 2008.

[38] E. W. Ng, D. T. Shima, P. Calias, E. T. Cunningham, D. R. Guyer, A. P. Adamis, "Pegaptanib, a targeted anti-VEGF aptamer for ocular vascular disease," *Nature Reviews Drug Discovery,* vol. 5, pp. 123-132, 2006.

[39] W. R. Freeman, I. Falkenstein, "Avastin and New Treatments for AMD: Where Are We?," *Retina,* vol. 26, pp. 853-858, 2006.

[40] J. Gaudreault, J. Rusit, P. Suboc, V. Shiu, "Preclinical Pharmacokinetics of Ranibizumab (rhuFabV2) after a Single Intravitreal Administration," *Retina,* vol. 46, pp. 726-733, 2005.

[41] J. Lubkowski, A. Pluckthun, A. Wlodawer, "The structural basis of phage display elucidated by the crystal structure of the N-terminal domain of g3p," *Nature Structural Biology,* vol. 5, pp. 140-147, 1998.

[42] P. H. van Wezenbeek, T. J. Schoenmakers, "Nucleotide sequence of the filamentous bacteriophage M13 DNA genome: comparison with phage fd," *Gene,* vol. 11, pp. 129-148, 1980.

[43] T. P. Henry, "The proteins of bacteriophage M13," *Proceedings of the National Academy of Sciences,* vol. 62, pp. 800-807, 1969.

[44] M. J. Glucksman, "Three-dimensional structure of a cloning vector: X-ray diffraction studies of filamentous bacteriophage M13 at 7 Å resolution," *Journal of Molecular Biology,* vol. 226, pp. 455-470, 1992.

[45] W. W. Norton & Company, "Molecular Biology Of Viruses," in *Microbiology, 2nd edition* vol. 1, ed. W. W. Norton & Company, Inc.,

500 Fifth Avenue, New York, New York 10110: W. W. Norton & Company, Inc.

[46] D. J. Rodi, L. Makowski, "Phage-display technology – finding a needle in a vast molecular haystack," *Current Opinion in Biotechnology,* vol. 10, pp. 87-93, 1999.

[47] J. W. Crissman, G. P. Smith, "Gene-Ill Protein of Filamentous Phages: Evidence for a Carboxyl-Terminal Domain with a Role in Morphogenesis," *Virology,* vol. 132, pp. 445-455, 1984.

[48] L. Makowski, "Phagedisplay: structure, assembly and engineering of filamentous bacteriophageM13," *Current Opinion in Structural Biology,* vol. 4, pp. 225-230, 1994.

[49] V. A. Petrenko, V. J. Vodyanoy, "Phage display for detection of biological threat agents," *Journal of Microbiological Methods,* vol. 53, pp. 253-262, 2003.

[50] F. Felici, L. Castagnoli, A. Musacchio, R. Jappelli, G. Cesareni, "Selection of antibody ligands from a large library of oligopeptides expressed on a multivalent exposition vector," *Journal of Molecular Biology,* vol. 222, pp. 301-310, 1991.

[51] K. T. O'Neil, R. H. Hoess, "Phage display: protein engineering by directed evolution," *Current Opinion in Structural Biology,* vol. 5, pp. 443-449, 1995.

[52] G. A. Løset, B. Bogen, I. Sandlie, "Expanding the Versatility of Phage Display I: Efficient Display of Peptide-Tags on Protein VII of the Filamentous Phage," *PLoS ONE,* vol. 6, p. e14702, 2011.

[53] S. S. Sidhu, G. A. Weiss, J. A. Wells, "High copy display of large proteins on phage for functional selections1," *Journal of Molecular Biology,* vol. 296, pp. 487-495, 2000.

[54] S. S. Sidhu, G. Fuh, "Efficient phage display of polypeptides fused to the carboxy-terminus of the M13 gene-3 minor coat protein," *FEBS Letters,* vol. 480, pp. 231-234, 2000.

[55] D. A. Marvin, "Filamentous phage structure, infection and assembly," *Current Opinion in Structural Biology,* vol. 8, pp. 150-158, 1998.

[56] D.A. Marvin , L. C. Welsh, M.F. Symmons, W.R. Scott, S.K. Straus, "Molecular Structure of fd (f1, M13) Filamentous Bacteriophage Refined with Respect to X-ray Fibre Diffraction and Solid-state NMR Data Supports Specific Models of Phage Assembly at the Bacterial Membrane," *Journal of Molecular Biology,* vol. 355, pp. 294-309, 2006.

[57] J. Lubkowski, F. Henneke, A. Plückthun, A. Wlodawer, "Filamentous phage infection: crystal structure of g3p in complex with its coreceptor, the C-terminal domain of TolA," *Structure,* vol. 7, pp. 711-722, 1999.
[58] S. S. Sidhu, "Engineering M13 for phage display," *Biomolecular Engineering,* vol. 18, pp. 57-63, 2001.

[59] A. D. Griffiths, "Production of human antibodies using bacteriophage," *Current Opinion in Immunology,* vol. 5, pp. 263-267, 1993.

[60] P. J. Schatz, "Use of Peptide Libraries to Map the Substrate Specificity of a Peptide-Modifying Enzyme: A 13 Residue Consensus Peptide Specifies Biotinylation in Escherichia coli," *Nature Biotechnology,* vol. 11, pp. 1138-1143, 1993.

[61] M. D. Scholle, U. Kriplani, A. Pabon, K. Sishtla, M. J. Glucksman, B. K. Kay, "Mapping Protease Substrates by Using a Biotinylated Phage Substrate Library," *ChemBioChem,* vol. 7, pp. 834-838, 2006.

[62] A. Chapman-Smith, J. E. Cronan, "Molecular Biology of Biotin Attachment to Proteins," *The Journal of Nutrition,* vol. 129, pp. 4775-4845, 1999.

[63] N. M. Green, "Avidin and Streptavidin," *Methods in Enzymology,* vol. 184, pp. 51-67, 1990.

[64] Y. Chen, C. Wiesmann, G. Fuh, B. Li, H. W. Christinger, P. McKay, A. M. de Vos, H. B. Lowman., "Selection and analysis of an optimized anti-VEGF antibody: crystal structure of an affinity-matured Fab in complex with antigen," *Journal of Molecular Biology,* vol. 293, pp. 865-81, 1999.

[65] Y. Denizot, R. De Armas, F. Caire, J. J. Moreau, I. Pommepuy, V. Truffinet, F. Labrousse, "The Quantitative analysis of bFGF and VEGF by ELISA in human meningiomas," *Mediators of Inflammation,* vol. 2006, p. 36376-36378, 2006.

[66] C. Hornig, T. Behn, W. Bartsch, A. Yayon, and H. A. Weich, "Detection and quantification of complexed and free soluble human vascular endothelial growth factor receptor-1 (sVEGFR-1) by ELISA," *Journal of Immunological Methods,* vol. 226, pp. 169-177, 1999.

[67] H. A. Weich, H. Bando, M. Brokelmann, P. Baumann, M. Toi, B. Barleon, "Quantification of vascular endothelial growth factor-C (VEGF-C) by a novel ELISA," *Journal of Immunological Methods,* vol. 285, pp. 145-155, 2004.

[68] S. I. Stoeva, J. S. Lee, J. E. Smith, S. T. Rosen, C. A. Mirkin, "Multiplexed Detection of Protein Cancer Markers with Biobarcoded

Nanoparticle Probes," *Journal of the American Chemical Society,* vol. 128, pp. 8378-8379, 2006.

[69] K. Koski, J. Hölsä, P. Juliet, "Properties of aluminium oxide thin films deposited by reactive magnetron sputtering," *Thin Solid Films,* vol. 339, pp. 240-248, 1999.

[70] N. D. Hoivik, J. W. Elam, R. J. Linderman, V. M. Bright, S. M. George, Y. C. Lee, "Atomic layer deposited protective coatings for micro-electromechanical systems," *Sensors and Actuators A*, vol. 103, pp. 100-108, 2003.

[71] Q. L. Feng, T. N. Kim, J. Wu, E. S. Park, J. O. Kim, D. Y. Lim, "Antibacterial effects of Ag-HAp thin films on alumina substrates," *Thin Solid Films,* vol. 335, pp. 214-219, 1998.

[72] M. K. Tripp, C. Stampfer, D. C. Miller, T. Helbling, C. F. Herrmann, C. Hierold, "The mechanical properties of atomic layer deposited alumina for use in micro- and nano-electromechanical systems," *Sensors and Actuators A: Physical,* vol. 130-131, pp. 419-429, 2006.

[73] A. Khanna, D. G. Bhat, A. Harris, B. D. Beake, "Structure-property correlations in aluminum oxide thin films grown by reactive AC magnetron sputtering," *Surface and Coatings Technology,* vol. 201, pp. 1109-1116, 2006.

[74] J. M. Daughton, "Magnetoresistive Memory Technology," *Thin Solid Films,* vol. 216, pp. 162-168, 1992.

[75] S. J. Osterfeld, H. Yu, R. S. Gaster, S. Caramuta, L. Xu, S. J. Han, "Multiplex protein assays based on real-time magnetic nanotag sensing," *Proceedings of the National Academy of Sciences of the United States of America,* vol. 105, pp. 20637-20640, 2008.

[76] B. Lu, M. R. Smyth, R. O'Kennedy, "Tutorial review. Oriented immobilization of antibodies and its applications in immunoassays and immunosensors," *Analyst,* vol. 121, pp. 29-32, 1996.

[77] S. V. Rao, K. W. Anderson, L. G. Bachas, "Oriented immobilization of proteins," *Microchimica Acta,* vol. 128, pp. 127-143, 1998.

[78] M. Wikström, U. Sjobring, T. Drakenberg, S. Forsén, L. Björck, "Mapping of the Immunoglobulin Light Chain-binding Site of Protein L," *Journal of Molecular Biology,* vol. 250, pp. 128-133, 1995.